

## Aminoadamantanes with Persistent in Vitro Efficacy against H1N1 (2009) Influenza A

Antonios Kolocouris,<sup>\*,†</sup> Christina Tzitzoglaki,<sup>†</sup> F. Brent Johnson,<sup>‡</sup> Roland Zell,<sup>§</sup> Anna K. Wright,<sup>||</sup> Timothy A. Cross,<sup>||</sup> Ian Tietjen,<sup>⊥</sup> David Fedida,<sup>⊥</sup> and David D. Busath<sup>\*,#</sup>

<sup>†</sup>Department of Pharmaceutical Chemistry, Faculty of Pharmacy, National and Kapodistrian University of Athens, Athens 15771, Greece

<sup>‡</sup>Department of Microbiology and Molecular Biology, Brigham Young University, Provo, Utah 84602, United States

<sup>§</sup>Department of Virology and Antiviral Therapy, Jena University Hospital, CMB Building, R. 443, Hans Knoell Strasse 2, D-07745 Jena, Germany

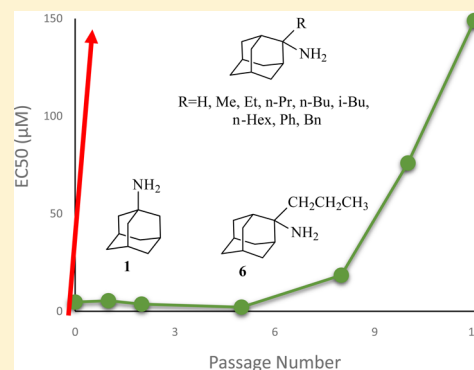
<sup>||</sup>Department of Chemistry and Biochemistry and National High Magnetic Field Laboratory, Florida State University, Tallahassee, Florida 32306, United States

<sup>⊥</sup>Department of Anesthesiology, Pharmacology and Therapeutics, University of British Columbia, Vancouver, British Columbia, V6T 1Z3, Canada

<sup>#</sup>Department of Physiology and Developmental Biology, Brigham Young University, Provo, Utah 84602, United States

### S Supporting Information

**ABSTRACT:** A series of 2-adamantanamines with alkyl adducts of various lengths were examined for efficacy against strains of influenza A including those having an S31N mutation in M2 proton channel that confer resistance to amantadine and rimantadine. The addition of as little as one CH<sub>2</sub> group to the methyl adduct of the amantadine/rimantadine analogue, 2-methyl-2-aminoadamantane, led to activity in vitro against two M2 S31N viruses A/Calif/07/2009 (H1N1) and A/PR/8/34 (H1N1) but not to a third A/WS/33 (H1N1). Solid state NMR of the transmembrane domain (TMD) with a site mutation corresponding to S31N shows evidence of drug binding. But electrophysiology using the full length S31N M2 protein in HEK cells showed no blockade. A wild type strain, A/Hong Kong/1/68 (H3N2) developed resistance to representative drugs within one passage with mutations in M2 TMD, but A/Calif/07/2009 S31N was slow (>8 passages) to develop resistance in vitro, and the resistant virus had no mutations in M2 TMD. The results indicate that 2-alkyl-2-aminoadamantane derivatives with sufficient adducts can persistently block p2009 influenza A in vitro through an alternative mechanism. The observations of an HA1 mutation, N160D, near the sialic acid binding site in both 6-resistant A/Calif/07/2009(H1N1) and the broadly resistant A/WS/33(H1N1) and of an HA1 mutation, I325S, in the 6-resistant virus at a cell-culture stable site suggest that the drugs tested here may block infection by direct binding near these critical sites for virus entry to the host cell.



### INTRODUCTION

Since 2005,<sup>1</sup> the amantadine/rimantadine-insensitive S31N mutation has become prevalent globally,<sup>2</sup> abrogating clinical usefulness of amantadine **1** and rimantadine **2**<sup>3</sup> and possibly previously developed M2 blocking compounds.<sup>4</sup> If the replacement of Ser31 with the larger Asn in M2 S31N splay the helix bundle at the drug binding site,<sup>5</sup> as suggested by solution state NMR studies,<sup>5d,6</sup> then drugs larger than rimantadine might be expected to be effective blockers. However, initial attempts to identify larger adamantane-based compounds that block amantadine-resistant viruses were unsuccessful.<sup>7</sup> Further efforts identified spiranamine analogues based on BL-1743<sup>8</sup> that were effective against V27A and L26F mutants<sup>9a</sup> but not against S31N, while other large templates could inhibit V27A<sup>9b-d</sup> but not S31N. Subsequently, reports of

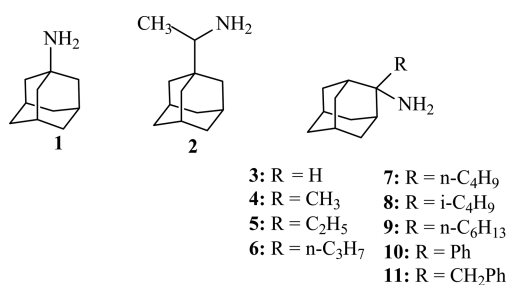
successful adamantane- and pinanamine-based M2 S31N blockers have appeared.<sup>6,10</sup> The design of these molecules was not based on the enlargement of the amantadine WT-M2 binding site, and the structural analysis of one active compound, comprising an amantadine linked through a methylene bridge to an isoxazole having an aryl substituent, showed that its heterocyclic ring may be trapped by the V27 side chains at the mouth of the channel.<sup>6</sup> Triggered by previous efforts aimed at adequately filling the empty expanded pore region due to the S31N mutation and to determine progressively the minimal variation of amantadine required to block influenza A (H1N1, M2 S31N), we evaluated drug

Received: January 16, 2014

Published: May 4, 2014

efficacy and mechanism for variations of amantadine **1** with alkyl adducts ranging from small to moderate and larger sizes (Scheme 1) as represented by the 2-alkyl-2-aminoadamantane

**Scheme 1. Amantadine 1, Rimantadine 2, and 2-Alkyl-2-aminoadamantane Derivatives 3–11**



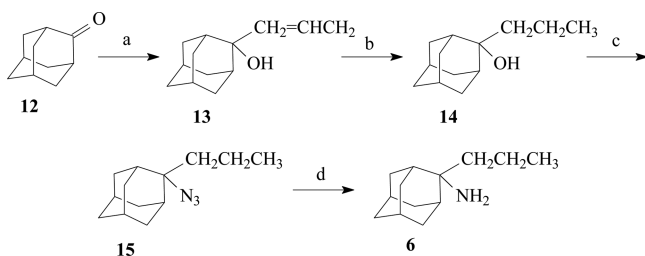
derivatives **3–11**, which are simpler than previously reported aminoadamantane derivatives active against S31N viruses<sup>10e</sup> and the larger of which have increased volume compared to amantadine.

We found with **5** that the addition of as little as one CH<sub>2</sub> group to the methyl adduct of the amantadine/rimantadine analogue, 2-methyl-2-aminoadamantane **4** (Scheme 1), recovers activity in vitro against the amantadine-resistant A/Calif/07/2009. However, the mechanism of action is not M2-block but a second aminoadamantane target.

## RESULTS AND DISCUSSION

**Chemistry.** Compounds **3–11** belong to the class of 2-alkyl-2-aminoadamantanes, which thus bear a substitution at adamantane C2 carbon. Compounds **3–6**<sup>4b</sup> and **10**<sup>11</sup> were previously synthesized but resynthesized with slightly modified procedures in this work. Tertiary alcohol **13** was obtained by treating 2-adamantanone **12** with allylmagnesium bromide (Scheme 2). The unsaturated alcohol **13** was converted to the

**Scheme 2. Preparation of 2-*n*-Propyl-2-aminoadamantane 6<sup>a</sup>**

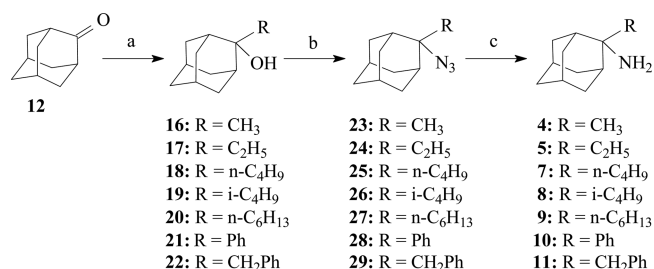


<sup>a</sup>Reagents and conditions: (a) CH<sub>2</sub>=CHCH<sub>2</sub>MgBr, ether, THF, rt, 2 h, then NH<sub>4</sub>Cl/H<sub>2</sub>O (quant); (b) H<sub>2</sub>/PtO<sub>2</sub> (quant); (c) NaN<sub>3</sub>, TFA, CH<sub>2</sub>Cl<sub>2</sub>, 0 °C, then rt (quant); (d) LiAlH<sub>4</sub>, ether, rt, 5 h (74%).

*n*-propyl derivative **14** through catalytic hydrogenation over PtO<sub>2</sub>. After experiments with tertiary alcohols in the adamantane series and an acyclic series (unpublished data), we concluded that the conversion of tertiary alcohols to the corresponding azides through NaN<sub>3</sub>/H<sub>2</sub>SO<sub>4</sub> (various concentrations)/CHCl<sub>3</sub><sup>4b,12</sup> or NaN<sub>3</sub>/TFA/CHCl<sub>3</sub><sup>11</sup> can result in unreacted alcohol and found that the transformation proceeds efficiently using NaN<sub>3</sub>/TFA 1 M in CH<sub>2</sub>Cl<sub>2</sub>. The amine **6** was prepared by means of LiAlH<sub>4</sub> reduction of the azide **15** in refluxing ether.

The amines **4, 5, 7–11** were synthesized according to Scheme 3. Tertiary alcohols **16–22** were obtained by treating

**Scheme 3. Preparation of 2-Alkyl-2-aminoadamantane Derivatives 4, 5, 7–11<sup>a</sup>**



<sup>a</sup>Reagents and conditions: (a) RLi, Ar, ether, THF, 0 °C, 2 h rt for **17–20** or RMgCl, ether, THF, 2 h rt for **16, 20, 21**, then NH<sub>4</sub>Cl/H<sub>2</sub>O (85–96%); (b) NaN<sub>3</sub>, TFA, CH<sub>2</sub>Cl<sub>2</sub>, 0 °C, then rt (50–96%); (c) LiAlH<sub>4</sub>, ether, rt, 5 h (23–65%).

2-adamantanone **12** with an organolithium (R = Et, *n*-Bu, *i*-Bu, *n*-hexyl) or organomagnesium reagent (R = Me,<sup>4b</sup> Ph, or PhCH<sub>2</sub>) (Scheme 3). While 2-methyl-2-adamantanol **16** was obtained after treating 2-adamantanone **12** with CH<sub>3</sub>MgI, this is not an efficient method for the preparation of alcohols **17–22** because of the bulky 2-adamantanone **12** and the soft carbanion character of the Grignard reagent making the β-hydride transfer a competitive reaction to the alkyl addition and leading to a mixture of the desired tertiary alcohol with 2-adamantanol. The conversion of tertiary alcohols **16–22** to the corresponding azides **23–29** was accomplished efficiently through treatment with NaN<sub>3</sub>/TFA 1 M in dichloromethane or dichloroethane for 24 h at room temperature. The primary *tert*-alkylamines **4, 5, 7–11** were prepared by means of LiAlH<sub>4</sub> reduction of the azides **23–29** in refluxing ether for 5 h.

**Solid State NMR of the M2 TMD Tetramer.** PISA wheel analysis gives a direct readout of helix tilt relative to the membrane normal for membrane proteins in uniformly oriented lipid bilayer preparations from solid state NMR PISEMA experiments.<sup>13</sup> <sup>15</sup>N anisotropic chemical shifts and <sup>15</sup>N–<sup>1</sup>H dipolar interactions observed in these spectra are very sensitive to the orientation of the peptide planes relative to the bilayer normal. Binding of compound **6** shifts the signals for three pertinent backbone amides that were isotopically labeled (Figure 1).

Binding of amantadine **1** to WT M2 TMD (A/Udorn/307/72 sequence) produces an 11° kink near G34 in each helix of the tetramer.<sup>5e</sup> When drug-bound, the helix tilt for the N-terminal half (residues 22–34) is 31° and in the C-terminal half (residues 35–46) just 20°.<sup>14</sup> Here, the S31N M2 TMD is labeled at two sites in the N-terminal half (residues V28 and A30) and one site in the C-terminal half (residue I42) of the TMD helix. The S31N data without drug suggest a helical tilt of approximately 36°, similar to that seen in the WT structure.<sup>5</sup> The shifts in the anisotropic spin interactions upon drug binding demonstrate a significant change in the structure of the tetrameric complex. With compound **6**, there is a uniform tilt of ~33°. Thus, the **6**-induced changes in the resonance frequencies of these three sites indicate that the tilt angle for the entire TMD helix is decreased by 3° while maintaining a similar rotational orientation for the helices. Unlike the response of the WT to amantadine **1**, with **6** the S31N TMD helices do not appear to have kinked the helix at G34. Instead,

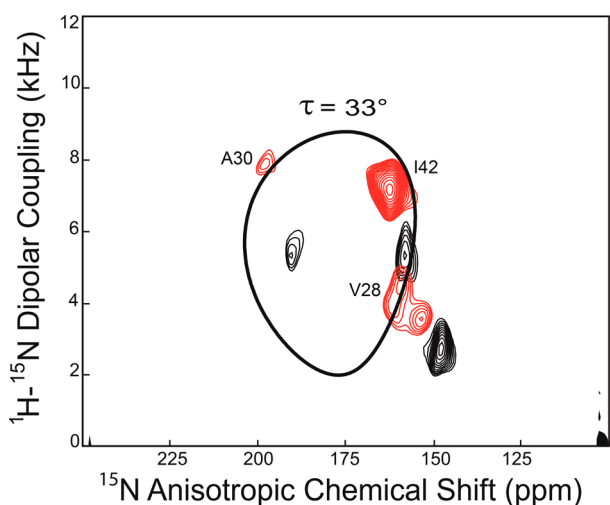


**Figure 1.** Superimposed PISEMA spectra of the S31N M2 transmembrane domain (residues 22–46),  $^{15}\text{N}$  labeled at residues V28, A30, and I42, in dimyristoylphosphatidylcholine bilayers uniformly aligned on glass slides with (red) and without (black) compound 6. Assignments were made based on the known structure and spectra of WT M2 TMD.<sup>15</sup> The assignments with drug follow based on the rotational orientation of the helices.

the entire helix–helix interface changes with the  $\sim 3^\circ$  reduction in tilt of the four helices. Similar results from ssNMR experiments and proteoliposome assays were obtained with two related aminoadamantanes that are not included in Scheme 1.

#### Electrophysiology Results Using Full-Length M2.

Representative compounds 3 and 6 were subsequently tested for block of proton currents through full-length M2 having the same amino acid sequence as A/California/07/2009 (*viz.*, S31N) using transiently transfected, voltage-clamped HEK cells<sup>16</sup> and found not to block inward proton currents on the 3 min time scale with any improvement over amantadine 1 (Table 1, Figure S1 in Supporting Information). Prolonged exposure (30 min) yielded but little increase in net block over 3 min exposure for the two drugs. When the M2 protein was reverted to the S31 WT sequence (through an N31S mutation), inward proton currents in M2-transfected HEK cells were well blocked by 1, 3, and 6. This electrophysiology result suggests (a) that these two drugs do not block the M2 S31N channel in full length A/Calif/07/2009 and must have a different target and (b) that biophysical models for the M2 protein should be based on the whole protein rather than segments. This conclusion supports other studies suggesting another target of aminoadamantane compounds.<sup>7,10e,g</sup> Similar results were also obtained with a few other related aminoadamantanes not included in this work.

**Biological Evaluation.** (a) *Antiviral Evaluation.*  $\text{EC}_{50}$  values from dose–response tests against five strains of influenza A in Madin–Darby canine kidney (MDCK) cells were measured using a primary infection assay (Table 2). This assay detects block at the early stages of viral replication, from endocytotic uptake to protein synthesis.

All compounds except 1–5 display potent antiviral activity against the pandemic 2009 strain (arbitrarily designated as <24  $\mu\text{M}$  based on the amantadine insensitivities observed here). It is striking that the addition of as little as one  $\text{CH}_2$  group to the methyl adduct of the amantadine/rimantadine analogue, 2-methyl-2-aminoadamantane 4, essentially recovers activity in vitro against this amantadine-resistant form of influenza A.

Likewise, the amantadine-resistant H1N1 strain from 1934 (second column), containing a double mutant M2 (T27 + N31), is highly sensitive to these compounds. But the drugs do not block all M2(S31N)-bearing or all H1N1 strains<sup>10e</sup> as shown by the third column, which shows that the 1933 Wilson Smith H1N1 isolate is insensitive to most of these compounds. Furthermore, the M2 pore region (residues 22–46) of A/WS/33 and A/Calif/2009 are identical except for the L43T variation at the C-terminus (Supporting Information Table 1). These observations are consistent with the negative electrophysiology results for the A/Calif/2009/M2, further suggesting that the antiviral effects observed against the A/Calif/2009 strain are independent of M2 and that instead they attack a second target.<sup>7,10g</sup> This second target is most likely present in A/Calif/07/2009 and probably in A/PR/8/34 but not in A/WS/33. Strains with WT M2 are very sensitive to these compounds (fourth and fifth columns), suggesting that, like amantadine, these drugs also block M2. However, from the structure–activity point of view, differences between the sequence and optimal efficacies vary, suggesting that nonbinding site residue differences in the M2 may alter efficacy. For instance 6 is the one of the most potent in the set against A2/Taiwan/1/64 H2N2 but the least potent of the set against A/Victoria/3/75 H3N2, even though both have WT-M2 amantadine-binding sites. They differ in only two residues, 13 and 56, neither of which is in the pore region (Supporting Information Table 1). This suggests that extra-pore residues may affect M2 block. On the other hand, 9 is the most effective from the set against all of the strains tested except A2/Taiwan/1/64, where it is among the least effective, which may suggest that the relative impacts of M2 block and any alternative mechanisms of action are also dependent on drug structure.

(b) *Resistance Experiments: Sequencing of Resistant Strains.* Resistance testing with semiweekly passages in MDCK cell cultures was performed for amantadine 1 against an amantadine-sensitive H3N2 virus and for compound 6 against amantadine-resistant H1N1 (2009) (Table 3).

In the amantadine–H3N2 system, drug resistance appeared after one passage in the presence of drug, with no detectable

**Table 1. Proton Channel Block Measured in Transfected HEK Cells for Compounds Tested<sup>a</sup>**

compd	A/England/195/2009 (H1N1), <sup>b</sup> M2/N31		A/England/195/2009 (H1N1), M2/S31	
	% block after 3 min	% block after 30 min	% block after 3 min	$\text{IC}_{50}$ , $\mu\text{M}$
1	14 $\pm$ 2 (100 $\mu\text{M}$ ; 26)	(N/A)	75 $\pm$ 9 (10 $\mu\text{M}$ ; 4)	1.6 $\pm$ 2.7 (3)
3	13 $\pm$ 3 (100 $\mu\text{M}$ ; 2)	16 (100 $\mu\text{M}$ ; 1)	95 $\pm$ 8 (10 $\mu\text{M}$ ; 2)	2.5 $\pm$ 0.5 (2)
6	0 $\pm$ 5 (100 $\mu\text{M}$ ; 2)	9.4 $\pm$ 10 (100 $\mu\text{M}$ ; 3)	63 $\pm$ 5 (10 $\mu\text{M}$ ; 2)	7 $\pm$ 2 (2)

<sup>a</sup>For each compound, % block of pH-dependent M2 current at 10 or 100  $\mu\text{M}$  ( $\pm\text{SEM}$ ) or the  $\text{IC}_{50}$  ( $\mu\text{M}$ ) is shown. Number of replicates is shown in parentheses. <sup>b</sup>The M2 sequence for this strain is identical to that of A/Calif/07/2009 M2.



Table 2. In Vitro Efficacy ( $EC_{50}$ ,  $\mu M$ ) of Scheme 1 Compounds against Initial MDCK Cell Infection<sup>a</sup>

compd	A/Calif/07/09 (H1N1)	A/PR/8/34 (H1N1)	A/WS/33 (H1N1)	A2/Taiwan/1/64 (H2N2)	A/Victoria/3/75 (H3N2)
M2	S31N	V27T/S31N	S31N	WT	WT
1	240 ± 90 (13)	24 ± 3.5 (21)	24 ± 1.1 (21)	0.34 ± 0.01 (21)	2.8 ± 0.3 (16)
2	110 ± 40 (13)	3.3 ± 0.5 (2)	310 ± 140 (2)	1.6 ± 0.3 (2)	0.53 ± 0.07 (18)
3	150 ± 30 (20)	3.8 ± 1.0 (2)	110 ± 15 (2)	0.8 ± 0.3 (2)	3.3 ± 0.9 (2)
4	54 ± 2 (20)	0.4 ± 0.4 (2)	19 ± 4 (2)	0.5 ± 0.5 (2)	2.0 ± 0.4 (2)
5	25 ± 3 (21)	1.8 ± 0.9 (2)	23 ± 3 (2)	0.8 ± 0.3 (2)	2.0 ± 0.4 (2)
6	4.7 ± 0.9 (20)	0.5 ± 0.2 (2)	390 ± 8 (2)	<0.24 (2)	23 ± 8 (2)
7	8.5 ± 0.6 (20)	0.3 ± 0.3 (2)	355 ± 4 (2)	1.5 ± 0.3 (2)	4 ± 1 (2)
8	8.0 ± 0.3 (21)	0.3 ± 0.5 (2)	210 ± 40 (2)	0.4 ± 0.1 (2)	13 ± 2 (2)
9	0.13 ± 0.02 (2)	0.07 ± 0.09 (2)	13.0 ± 3.6 (2)	1.5 ± 0.3 (2)	1.1 ± 0.1 (2)
10	21 ± 2 (21)	<0.3 ± 0.5 (2)	86 ± 20 (2)	0.2 ± 0.2 (2)	8 ± 1 (21)
11	8.6 ± 0.8 (21)	1.2 ± 1.1 (2)	280 ± 150 (2)	0.2 ± 0.3 (2)	18 ± 2 (21)

<sup>a</sup> $EC_{50} \pm$  its standard error ( $N$ ) from miniplaque testing for dose–response or single-dose screens, using cultured MDCK cells, based on least-squares fitting of single-site binding curves.  $N$  is the number of assay counts fitted. Experiments with  $N = 2$  are based on replicate 50  $\mu M$  screens (except for 9, which were based on replicate 5  $\mu M$  screens), with a single control ( $N = 4$ ) for each virus. Row M2 gives variations from the WT amantadine-binding site (i.e., L26, V27, A30, S31, and G34) for the specific strain listed, WT if none. (See Tables S3, S4, and S5 for the M2 sequences of the isolates used here.) No microscopic evidence of cytotoxicity to MDCK cells was detected after an 18 h exposure at 50  $\mu M$  except with compound 9, where a 5  $\mu M$  dose was used instead. The  $EC_{50}$  values of amantadine 1 and rimantadine 2, known to be inactive against H1N1 (2009), and other cases where  $EC_{50} \geq 24 \mu M$  are highlighted.

Table 3. Resistance Testing of Amantadine 1 and 2-*n*-Propyl-2-aminoadamantane 6<sup>a</sup>

passage no.	$EC_{50} \pm SE$ ( $\mu M$ )	
	1 (5 $\mu M$ ), A/Victoria/3/75 (H3N2, M2 WT)	6 (5 $\mu M$ ), A/Calif/07/2009 (H1N1, M2 S31N)
0	2.77 ± 0.29	4.71 ± 0.92
1	inactive	5.4 ± 1.4
2	inactive	3.7 ± 0.5
5	ND	2.1 ± 1.6
8	ND	18.5 ± 1.0
10	ND	76 ± 9
12	ND	149 ± 115

<sup>a</sup> $EC_{50} \pm SE$  ( $\mu M$ ) ( $N = 21$ ) after designated passage (incubation) stages. Drug concentration in medium as specified except that for 6, passages 1 and 2 were done in 10  $\mu M$ . Inactive: no miniplaque reduction by 50  $\mu M$  amantadine. ND: not done.

activity of amantadine 1 against the progeny from passage 1 or passage 2 at 50  $\mu M$  but normal amantadine 1 activity against the original virus post hoc ( $EC_{50} = 3.0 \pm 0.5 \mu M$ ;  $N = 9$ ). In contrast, in the 6–H1N1 system, virus progeny produced in the presence of drug at passages 1–5 maintained full drug sensitivity ( $EC_{50} = 2.1–5.4 \mu M$ ). Resistance to 6 developed steadily between passage 6 and passage 12, becoming significant after passage 10. Without any drug in the medium, the development of viral resistance to compound 6 was negligible; i.e., the  $EC_{50}$  retested at passage 0 was  $4.7 \pm 0.7 \mu M$ , at passage 10 was  $3.0 \pm 0.3$ , and at passage 30 was  $7.7 \pm 0.6 \mu M$ . Resistance to amantadine develops rapidly in vitro,<sup>17</sup> in mice,<sup>18</sup> and in the clinical setting<sup>19</sup> through a small set of mutations, primarily L26F, V27A, V27T, A30T, S31N, and G34E.<sup>20</sup> These are residues whose side chains are near the 4-fold symmetric amantadine binding site.<sup>5</sup> No changes from the parent A/California/07/2009 were observed for the amino acid translation of the M-segment of the passage-12 6-resistant strain for residues sequenced, 10–73. Hence, resistance did not develop by selection of additional amantadine-resistance mutations in M2. Sequencing of segment 4 (HA gene), however, revealed three amino acid substitutions (Figure 2, Table S1) compared to the parental A/California/07/2009 sequence, i.e., N160D,

S187P, and I325S (numbering started after the 13-residue HA signal sequence).

To evaluate whether these mutations were merely due to adaptation to MDCK cell culture growth, we also sequenced the M (Tables S2 and S3) and HA segments (Table S1) from the parent virus after 30 passages in MDCK culture without drug. For the M segment of these drug-free controls, no changes were found in M1, while 2 of 5 plaques had an E14G

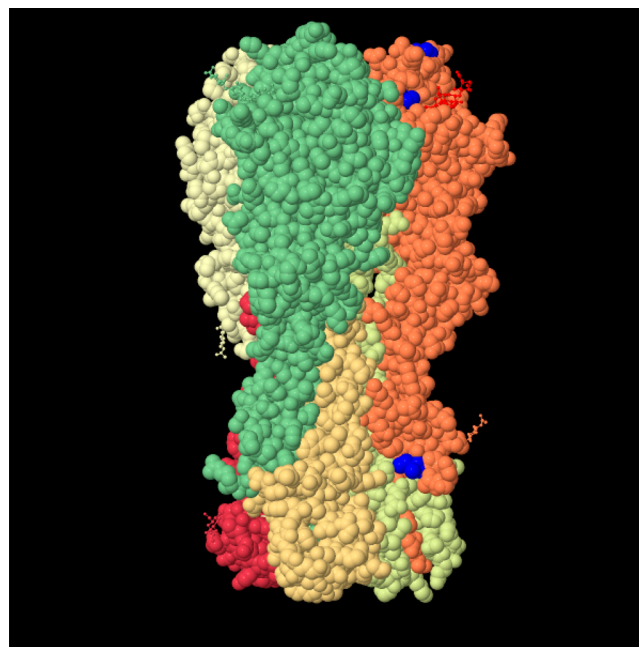


**Figure 2.** CPT structure of the HA trimer, produced by Gamblin et al. (1RVX, A/Puerto Rico/8/1934)<sup>21</sup> with a bound NAG-GAL-SIA ligand as ball-and-stick (red) and with the two nearby 6-resistance sites highlighted in blue, residues 159 (above ligand) and 186 (left of ligand). The third 6-resistance site, 324, also in blue, is near the bottom of the structure. Because of a common insertion after residue 133 found in A/Calif/07/2009 (H1N1), these correspond to N160, S187, and I325, respectively, in the A/Calif/07/2009 6-resistant mutants.

substitution in M2, which is outside the transmembrane domain.

Substitution S187P, located near the N-terminus of the 190 sialic acid binding helix, is frequent in pandemic H1N1 and was observed previously by Torres et al. in resistance development using a related set of aminoadamantanes.<sup>10g</sup> In the drug-free controls, 2 out of 5 plaques showed this mutation, as well as 1 of 4 previously sequenced isolates of A/California/07/2009 (KF00954, Table S1).

N160 is located on the tip of a nearby loop that is very close to the 190 helix, the region where sialic acid residues of the host cell receptor bind. Among 1750 HA sequences of pandemic H1N1 deposited in the GenBank only four sequences with D160 were observed. Substitution of N160 by an aspartic acid residue would modify the local charges and may thus affect receptor interactions. Interestingly, D160 is also observed in A/WS/33, which may account for the insensitivity of this strain to the compounds tested here (Table 1). However, in the drug-free controls, 1 of 5 plaques tested had this mutation (Table S1). Three other plaques had the G159E mutation, suggesting that an acidic group in that neighborhood is advantageous for the pandemic virus replication in MDCK culture. On the other hand that mutation is also present in our sample of the highly 6-sensitive A/PR/8/34 strain (Table S1), suggesting that if D160 is critical for drug inhibition, an acid group at position 159 is not sufficient for drug resistance. The possibility that N160D is important to escape from 6 cannot be ruled out.

S325 is close to the HA0 processing site at R331 and the corresponding residue, 324, was also found to be modified in the aminoadamantane resistance development study by Torres et al.<sup>10g</sup> None of the 1750 HA sequences of pandemic H1N1 in GenBank has a serine at position 325. This substitution may affect maturation cleavage or pH stability of HA. Although it was pointed out<sup>10g</sup> that a mutation to T at this site is found in one sequence of A/Puerto Rico/8/1934 and that this site may be polymorphic, we found seven sequences for that strain without the mutation and no I325T substitution was observed in our GenBank set of 1750 pandemic H1N1 strains. Furthermore, no instances of an I325 mutation were observed in the drug-free control virus plaques (Table S1). This suggests that drugs inhibit an important function at this site such as enzyme binding or cleavage.

To examine the resistance development pathways of the H3N2 M2 WT virus to these compounds in more detail, passaging experiments were carried out with plaque sequencing analysis in the presence of active compound 4 or 6 (Table 4). The WT virus rapidly develops resistance to both compounds through mutation at Ala30, especially to Thr, suggesting that these drugs block the M2 WT but do not block A30T. Conversely, the lack of sequence changes for M2(S31N)-bearing virus in the presence of compound 6 mentioned above indicates that M2(S31N)-bearing virus has a different escape route than M2(WT)-bearing virus. In the latter case changes inside the M2 pore confer resistance, while in the former no mutations were observed in the M2 channel amantadine binding site; therefore, some other change in the virus is implicated.

## CONCLUSION

The addition of as little as one CH<sub>2</sub> group to the methyl adduct of the amantadine/rimantadine analogue, 2-methyl-2-aminoadamantane 4, has been discovered to largely recover activity in vitro against the amantadine-resistant 2009 H1N1 influenza A.

**Table 4. Mutations Developing in Influenza A (M2 WT)<sup>a</sup> after Passaging in Aminoadamantane Derivatives 4 and 6<sup>b</sup>**

passage no. <sup>d</sup>	plaque no.	compd <sup>c</sup>	
		4, 1 μg/mL	6, 5 μg/mL
2	1	WT	A30T
	2	WT	A30T
	3	WT	A30T
5	1	A30T	A30T
	2	A30V	A30T
	3	A30T	A30T

passage no. <sup>d</sup>	plaque no.	compd <sup>c</sup>	
		4, 2 μg/mL	6, 5 μg/mL
10	1	A30T	A30T
	2	A30T	A30T
	3	A30T	A30T

<sup>a</sup>Parent strain: A/Hong Kong/1/1968 (H3N2M2 WT). <sup>b</sup>Sequences of resistant progeny of WT induced by compounds in the top row. MDCK cells were bathed in medium containing the concentrations specified. Three separate plaques were sampled and sequenced at passages 2, 5, and 10. <sup>c</sup>Compound number from Scheme 1. <sup>d</sup>Passage number.

The apparent simplicity of the synthetic schemes is a virtue of 2-alkyl-2-aminoadamantane derivatives. Resistance development in cell culture is markedly reduced for one representative compound 6 (R = *n*-Pr) compared to amantadine 1. These compounds found to be active against two of three S31N strains (A/Calif/07/009 and A/PR/8/34 but not A/WS/33) did not block M2, judging by the lack of transfected HEK cell current block and the lack of M2 changes in the 6-resistant A/Calif/07/2009, and therefore must have acted on a second target. The ssNMR study that confirmed that drugs with large alkyl adducts were sterically suited to fit in the amantadine binding site in M2 were done at effectively high drug concentrations and using truncated M2 protein (22–46) and do not indicate the potential of drugs to block the S31N variant of M2.

A few alternative candidate mechanisms of action for these drugs include pH buffering of the endosome, pH buffering of the viral interior, stabilization of hemagglutinin against acid activation, and mechanical stabilization at lipid–water interfaces against envelope–endosomal membrane fusion. The observations of an HA1 mutation, N160D, near the sialic acid binding site in both 6-resistant A/Calif/07/2009(H1N1) and the broadly resistant A/WS/33(H1N1) and of an HA1 mutation I325S in the 6-resistant virus at a cell-culture stable site suggest that the drugs tested here may block infection by direct binding near these critical sites. The region near residue 160 is critical for binding virus to the cell surface, and the region near residue 325 is critical for HA activation by proteolytic cleavage, both necessary for the virus entry into the host cell. It is also possible that the drugs neutralize the endosome and that these sites, individually or in combination, affect pH sensitivity of HA, as has been suggested in similar situations previously.<sup>7,10g</sup> However, miniplaque assays with compounds 3–6 against influenza B/Russia/69 in MDCK cells and compound 6 against bovine parvovirus in bovine embryonic cells, respectively, both of which are chloroquine sensitive,<sup>22,23</sup> showed no effect of 3–6 or 6, respectively, on virus growth with 50 μM drug in the medium (data not shown), suggesting that these compounds are less potent endosome neutralizers than chloroquine.

Further experiments are needed to explore these and other possibilities.

Continued outbreaks of amantadine-resistant viruses like H7N9 merit the urgency to develop new antivirals with persistent efficacy in global preparations for pandemic threats.<sup>24</sup> The new observation of persistent efficacy of these amantadine-like drugs via second targets, while retaining potency (albeit resistance vulnerable) to WT M2, makes this family of compounds intriguing starting points for further studies on resistance and mechanism of action against influenza A.

## EXPERIMENTAL SECTION

**(A) Chemistry.** Melting points were determined using a Buchi capillary apparatus and are uncorrected. IR spectra were recorded on a Perkin-Elmer 833 spectrometer. <sup>1</sup>H and <sup>13</sup>C NMR spectra were recorded on a Bruker DRX 400 and AC 200 spectrometer at 400 and 50 MHz, respectively, using CDCl<sub>3</sub> as solvent and TMS as internal standard. Carbon multiplicities were established by DEPT experiments. The 2D NMR techniques (HMQC and COSY) were used for the elucidation of the structures of intermediates and final products.

Microanalyses were carried out by the Service Central de Microanalyse (CNRS), France, and by the Microanalyses lab of the National Center for Scientific Research, Demokritos, Athens, Greece, and the results obtained had a maximum deviation of ±0.4% from the theoretical value. All tested synthesized compounds possess a purity above 95% as determined through elemental C, H, N analysis.

Full experimental details that were not given previously for compounds 4 and 5<sup>4b</sup> are included in this paper.

**2-Ethyltricyclo[3.3.1.1<sup>3,7</sup>]decan-2-amine (5).** 2-Ethyl-2-adamantanol 17 was obtained after treating a solution of 2-adamantanone 12 (500 mg, 3.34 mmol) in dry THF (10 mL, 30% solution w/v) with *n*-ethylolithium at 0 °C in a 3.7 molar excess (25 mL, 12.5 mmol, 0.5 M in benzene) and stirring the mixture overnight: yield 94%; <sup>1</sup>H NMR (CDCl<sub>3</sub>, 400 MHz) δ 0.86 (t, *J* = 7 Hz, CH<sub>2</sub>CH<sub>3</sub>), 1.40–1.70 (m, 10 H, 1',3'-H, 4'eq, 9'eq-H, 6'-H, 8'eq,10'eq-H, CH<sub>2</sub>CH<sub>3</sub>), 1.75–1.83 (m, 2H, 5',7'-H), 1.94 (d, *J* = 12 Hz, 2H, 8'ax, 10'ax-H), 2.07 (d, *J* = 12 Hz, 2H, 4'ax, 9'ax-H); <sup>13</sup>C NMR (CDCl<sub>3</sub>, 50 MHz) δ 6.4 (CH<sub>2</sub>CH<sub>3</sub>), 27.4, 27.5 (5',7'-C), 30.6 (CH<sub>2</sub>CH<sub>3</sub>), 33.0 (8',10'-C), 34.6 (4',9'-C), 36.6 (1',3'-C), 38.5 (6'-C), 74.9 (2'-C).

To a stirred mixture of NaN<sub>3</sub> (0.195 g, 3.0 mmol) and dry dichloromethane (5 mL) at 0 °C, TFA (1.14 g, 10.0 mmol) was added. To the stirred mixture, a solution of 2-ethyl-2-adamantanol 17 (0.180 g, 1.0 mmol) in dry dichloromethane (5 mL) was added, and stirring was maintained at 0 °C for 4 h. The mixture was stirred at ambient temperature for 24 h and then was treated with NH<sub>3</sub> 12% (30 mL) at 0 °C. The organic phase was separated, and the aqueous phase was extracted twice with an equal volume of dichloromethane. The combined organic phase was washed with water and brine, dried (Na<sub>2</sub>SO<sub>4</sub>), and evaporated to afford oily 2-ethyl-2-adamantylazide 24: IR (Nujol)  $\nu$ (N<sub>3</sub>) 2100 cm<sup>-1</sup>; yield 0.160 g (80%).

To a stirred suspension of LiAlH<sub>4</sub> (0.120 g, 0.78 mmol) in dry ether (10 mL) was added, dropwise at 0 °C, a solution of the 2-ethyl-2-adamantylazide 24 (0.160 g, 3.12 mmol) in dry ether (5 mL). The reaction mixture was refluxed for 5 h (TLC monitoring) and then hydrolyzed with water and NaOH (15%) and water under ice cooling. The inorganic precipitate was filtered off and washed with ether, and the filtrate was extracted with HCl (6%). The aqueous layer was made alkaline with solid Na<sub>2</sub>CO<sub>3</sub>, and the mixture was extracted with ether. The combined ether extracts were washed with water and brine and dried (Na<sub>2</sub>SO<sub>4</sub>). After evaporation of the solvent the oily amine 5 was obtained: yield 100 mg (71%); <sup>1</sup>H NMR (CDCl<sub>3</sub>, 400 MHz) δ 0.85 (t, *J* = 7 Hz, 3H, CH<sub>3</sub>), 1.55 (br s, 2H, 1',3'-H), 1.58–1.68 (m, 6H, 4'eq, 9'eq-H, 8'eq 6'-H), 1.78 (br s, 1H, 5'-H), 1.81 (br s, 1H, 7'-H), 1.93 (d, *J* = 12 Hz, 2H, 8'ax, 10'ax-H), 2.06 (d, *J* ≈ 12 Hz, 2H, 4'ax, 9'ax-H); <sup>13</sup>C NMR (CDCl<sub>3</sub>, 50 MHz) δ 6.5 (CH<sub>2</sub>CH<sub>3</sub>), 27.2, 27.6 (5',7'-C), 30.7 (CH<sub>2</sub>CH<sub>3</sub>), 33.0 (4',9'-C), 33.8 (8',10'-C), 36.6 (1',3'-C), 38.5 (6'-C), 74.9 (2'-C). Hydrochloride: mp >250 °C (EtOH–Et<sub>2</sub>O).

Anal. Calcd for C<sub>12</sub>H<sub>22</sub>NCl: C, 66.80; H, 10.28; N, 6.49. Found: C, 66.93; H, 10.42; N, 6.87.

**2-*n*-Propyltricyclo[3.3.1.1<sup>3,7</sup>]decan-2-amine (6).** Tertiary alcohol 13 was obtained after treating adamantanone 12 (1.0 g, 6.67 mmol) with CH<sub>2</sub>CH=CH<sub>2</sub>MgBr in 1:2 ratio (obtained from CH<sub>2</sub>CH=CH<sub>2</sub>Br (1.61 g, 13.3 mmol), 1.5 molar excess of Mg (486 mg, 20.01 mmol) in 20 mL of dry ether/g bromobenzene): yield 89%; <sup>1</sup>H NMR δ 1.52 (d, *J* = 12 Hz, 2H, 4'eq, 9'eq-H), 1.53–1.90 (m, 10H, adamantane-H), 2.15 (d, *J* = 12 Hz, 1H, 4'ax, 9'ax-H), 2.40 (d, *J* = 6 Hz, 2H, CH<sub>2</sub>CH=CH<sub>2</sub>), 5.05–5.15 (m, 2H, CH<sub>2</sub>CH=CH<sub>2</sub>), 5.75–6.0 (m, 1H, CH<sub>2</sub>CH=CH<sub>2</sub>). The unsaturated alcohol 13 (890 mg, 4.64 mmol) was hydrogenated under PtO<sub>2</sub> (45 mg) (catalyst was used in 1/20 percentage to the weight of the unsaturated compound) to afford the *n*-propyl analogue 14: yield, quant; <sup>1</sup>H NMR (CDCl<sub>3</sub>, 400 MHz) δ 0.92 (t, *J* = 7 Hz, 3H, CH<sub>3</sub>), 1.30–1.40 (m, 2H, CH<sub>2</sub>CH<sub>2</sub>CH<sub>3</sub>), 1.52 (d, *J* = 12 Hz, 2H, 4'eq, 9'eq-H), 1.58–1.61 (m, 2H, CH<sub>2</sub>CH<sub>2</sub>CH<sub>3</sub>), 1.68 (d, *J* = 12 Hz, 2H, 8'eq, 10'eq-H), 1.67 (br s, 2H, 6'-H), 1.68 (br s, 2H, 1', 3'-H), 1.79 (m, 2H, 5', 7'-H), 1.83 (d, *J* = 12 Hz, 2H, 8'ax, 10'ax-H), 2.16 (d, *J* = 12 Hz, 2H, 4'ax, 9'ax-H); <sup>13</sup>C NMR (CDCl<sub>3</sub>, 50 MHz) δ 14.9 (CH<sub>3</sub>), 15.4 (CH<sub>2</sub>CH<sub>2</sub>CH<sub>3</sub>), 27.4, 27.6 (5, 7-C), 33.1 (CH<sub>2</sub>CH<sub>2</sub>CH<sub>3</sub>), 34.7 (4, 9-C), 37.1 (8, 10-C), 38.5 (1, 3-C), 40.9 (6-C), 75.2 (2-C).

The alcohol 14 (700 mg, 4.22 mmol) was added to a stirred mixture of H<sub>2</sub>SO<sub>4</sub> 70% w/w (10 mL) and chloroform (25 mL) at 0 °C. Sodium azide was added in small portions at 0 °C, and the mixture was stirred for 48 h at ambient temperature. The mixture was poured into an ice–water mixture and was extracted with dichloromethane. The organic phase was washed with water, saturated NaHCO<sub>3</sub>, and brine, dried (Na<sub>2</sub>SO<sub>4</sub>), and evaporated under vacuum at room temperature. The oily residue (650 mg) was flash-chromatographed on silical gel (35–70 μm) with hexane–AcOEt 5/1 as an eluent to give the pure azide 15: yield 530 mg (66%). The azide 15 was found to form quantitatively using TFA/CH<sub>2</sub>Cl<sub>2</sub>/NaN<sub>3</sub> system (1 mmol of alcohol 14 was treated with 10 mmol of TFA and 4 mmol of NaN<sub>3</sub> in 40 mL of CH<sub>2</sub>Cl<sub>2</sub>; see experimental procedure for ethyl- or 2-*n*-butyltricyclo[3.3.1.1<sup>3,7</sup>]decan-2-azide 24 or 25): <sup>1</sup>H NMR (CDCl<sub>3</sub>, 400 MHz) δ 0.96 (t, *J* = 7 Hz, 3H, CH<sub>3</sub>), 1.42 (m, 2H, CH<sub>2</sub>CH<sub>2</sub>CH<sub>3</sub>), 1.59 (d, *J* = 12 Hz, 2H, 4'eq, 9'eq-H), 1.68–2.03 (m, 12H, CH<sub>2</sub>CH<sub>2</sub>CH<sub>3</sub>, adamantane-H), 2.10 (d, *J* = 12 Hz, 1H, 4'ax, 9'ax-H); <sup>13</sup>C NMR (CDCl<sub>3</sub>, 50 MHz) δ 14.7 (CH<sub>3</sub>), 16.4 (CH<sub>2</sub>CH<sub>2</sub>CH<sub>3</sub>), 27.2, 27.4 (5, 7-C), 33.8 (CH<sub>2</sub>CH<sub>2</sub>CH<sub>3</sub>), 34.4 (4, 9-C), 37.9 (8, 10-C), 38.5 (1, 3-C), 40.0 (6-C), 69.7 (2-C).

To a stirred suspension of LiAlH<sub>4</sub> (390 mg, 10.3 mmol) in dry ether (20 mL) was added, dropwise at 0 °C, a solution of the azide 15 (490 mg, 2.57 mmol) in dry ether (10 mL). The reaction mixture was refluxed for 5 h (TLC monitoring) and then hydrolyzed with water and NaOH (15%) and water under ice cooling. The inorganic precipitate was filtered off and washed with ether, and the filtrate was extracted with HCl (6%). The aqueous layer was made alkaline with solid Na<sub>2</sub>CO<sub>3</sub>, and the mixture was extracted with ether. The combined ether extracts were washed with water and brine and dried (Na<sub>2</sub>SO<sub>4</sub>). After evaporation of the solvent the oily amine 6 was obtained: yield 350 mg (74%); <sup>1</sup>H NMR (CDCl<sub>3</sub>, 400 MHz) δ 0.92 (t, *J* = 7 Hz, 3H, CH<sub>3</sub>), 1.29–1.40 (m, 2H, CH<sub>2</sub>CH<sub>2</sub>CH<sub>3</sub>), 1.52 (d, *J* = 12 Hz, 2H, 4'eq, 9'eq-H), 1.58–1.61 (m, 2H, CH<sub>2</sub>CH<sub>2</sub>CH<sub>3</sub>), 1.67 (d, *J* = 12 Hz, 2H, 8'eq, 10'eq-H), 1.66 (br s, 2H, 6'-H), 1.68 (br s, 2H, 1', 3'-H), 1.78 (br s, 2H, 5', 7'-H), 1.83 (d, *J* = 12 Hz, 2H, 8'ax, 10'ax-H), 2.16 (d, *J* = 12 Hz, 1H, 4'ax, 9'ax-H). Hydrochloride: mp > 250 °C (EtOH–Et<sub>2</sub>O). Anal. Calcd for C<sub>13</sub>H<sub>24</sub>NCl: C, 67.95; H, 10.53; N, 6.10. Found: C, 68.02; H, 10.63; N, 5.95.

**2-*n*-Butyltricyclo[3.3.1.1<sup>3,7</sup>]decan-2-amine (7).** Tertiary alcohol 18 was obtained after treating a solution of adamantanone 12 (500 mg, 3.34 mmol) in dry THF (30% solution w/v) with 3 molar excess of *n*-butyllithium (6 mL, 10.02 mmol, 1.6 M in hexanes) at 0 °C and stirring the mixture overnight: yield 96%; <sup>1</sup>H NMR (CDCl<sub>3</sub>, 400 MHz) δ 0.91 (t, *J* = 7 Hz, 3H, CH<sub>3</sub>), 1.25–1.38 (m, 4H, CH<sub>3</sub>CH<sub>2</sub>CH<sub>2</sub>CH<sub>2</sub>), 1.54 (d, *J* = 12 Hz, 2H, 4'eq, 9'eq-H), 1.58–1.72 (m, 8H, 1', 3', 5', 7', 8'eq, 10'eq-H, CH<sub>3</sub>CH<sub>2</sub>CH<sub>2</sub>CH<sub>2</sub>), 1.78–1.90 (m, 4H, 8'ax, 10'ax-H, 5',7'-H), 2.16 (d, *J* = 12 Hz, 1H, 4'ax, 9'ax-H); <sup>13</sup>C NMR (CDCl<sub>3</sub>, 50 MHz) δ 14.3 (CH<sub>3</sub>), 23.5



(CH<sub>2</sub>CH<sub>2</sub>CH<sub>2</sub>CH<sub>3</sub>), 24.4 (CH<sub>2</sub>CH<sub>2</sub>CH<sub>2</sub>CH<sub>3</sub>), 27.4, 27.6 (5',7'-C), 34.7 (4',9'-C), 33.1 (8',10'-C), 37.1 (1',3'-C), 38.2 (CH<sub>2</sub>CH<sub>2</sub>CH<sub>2</sub>CH<sub>3</sub>), 38.5 (6'-C), 75.2 (2'-C).

To a stirred mixture of NaN<sub>3</sub> (280 mg, 4.32 mmol) and dry dichloromethane (20 mL) at 0 °C, TFA (1.6 mg, 14.4 mmol) was added. To the stirred mixture, a solution of tertiary alcohol **18** (300 mg, 1.44 mmol) in dry dichloromethane (10 mL) was added, and stirring was maintained at 0 °C for 4 h. The mixture was stirred at ambient temperature for 24 h and then was treated with NH<sub>3</sub> 12% (30 mL) at 0 °C. The organic phase was separated, and the aqueous phase was extracted twice with an equal volume of dichloromethane. The combined organic phase was washed with water and brine, dried (Na<sub>2</sub>SO<sub>4</sub>), and evaporated to afford oily azide **25**: yield 96%; IR (Nujol)  $\nu$ (N<sub>3</sub>) 2088 cm<sup>-1</sup>; <sup>1</sup>H NMR (CDCl<sub>3</sub>, 400 MHz)  $\delta$  0.96 (t, *J* = 7 Hz, 3H, CH<sub>3</sub>), 1.32–1.42 (m, 4H, CH<sub>3</sub>CH<sub>2</sub>CH<sub>2</sub>CH<sub>2</sub>), 1.62 (d, *J* = 12 Hz, 2H, 4'eq, 9'eq-H), 1.70–1.93 (m, 12H, adamantane-H, CH<sub>3</sub>CH<sub>2</sub>CH<sub>2</sub>CH<sub>2</sub>), 2.14 (d, *J* = 12 Hz, 2H, 4'ax, 9'ax-H); <sup>13</sup>C NMR (CDCl<sub>3</sub>, 50 MHz)  $\delta$  14.2 (CH<sub>3</sub>), 23.3 (CH<sub>2</sub>CH<sub>2</sub>CH<sub>2</sub>CH<sub>3</sub>), 24.9 (CH<sub>2</sub>CH<sub>2</sub>CH<sub>2</sub>CH<sub>3</sub>), 27.2, 27.4 (5',7'-C), 33.8 (4',9'-C), 33.7 (8',10'-C), 34.4 (1',3'-C), 35.2 (CH<sub>2</sub>CH<sub>2</sub>CH<sub>2</sub>CH<sub>3</sub>), 38.5 (6'-C), 69.7 (2'-C).

To a stirred suspension of LiAlH<sub>4</sub> (163 mg, 4.29 mmol) in dry ether (15 mL) was added, dropwise at 0 °C, a solution of the azide **25** (250 mg, 1.07 mmol) in dry ether (10 mL). The reaction mixture was refluxed for 5 h (TLC monitoring) and then hydrolyzed with water and NaOH (15%) and water under ice cooling. The inorganic precipitate was filtered off and washed with ether, and the filtrate was extracted with HCl (6%). The aqueous layer was made alkaline with solid Na<sub>2</sub>CO<sub>3</sub>, and the mixture was extracted with ether. The combined ether extracts were washed with water and brine and dried (Na<sub>2</sub>SO<sub>4</sub>). After evaporation of the solvent the oily amine **7** was obtained: yield 50 mg (23%); <sup>1</sup>H NMR (CDCl<sub>3</sub>, 400 MHz)  $\delta$  0.88 (t, *J* = 7 Hz, 3H, CH<sub>3</sub>), 1.18–1.32 (m, 4H, CH<sub>3</sub>CH<sub>2</sub>CH<sub>2</sub>CH<sub>2</sub>), 1.45–1.65 (m, 10H, adamantane-H, CH<sub>3</sub>CH<sub>2</sub>CH<sub>2</sub>CH<sub>2</sub>), 1.77 (br s, 2H, 5',7'-H), 1.93 (d, *J* = 12 Hz, 2H, 8'ax, 10'ax-H), 2.03 (d, *J* = 12 Hz, 2H, 4'ax, 9'ax-H), 2.13 (br s, 2H, NH<sub>2</sub>); <sup>13</sup>C NMR (CDCl<sub>3</sub>, 50 MHz)  $\delta$  14.3 (CH<sub>3</sub>), 23.7 (CH<sub>2</sub>CH<sub>2</sub>CH<sub>2</sub>CH<sub>3</sub>), 24.6 (CH<sub>2</sub>CH<sub>2</sub>CH<sub>2</sub>CH<sub>3</sub>), 27.5, 27.8 (5',7'-C), 34.1 (4',9'-C), 33.2 (8',10'-C), 37.5 (1',3'-C), 38.6 (6'-C), 39.1 (CH<sub>2</sub>CH<sub>2</sub>CH<sub>2</sub>CH<sub>3</sub>), 54.5 (2'-C). Fumarate: mp 220 °C (EtOH–Et<sub>2</sub>O). Anal. Calcd for C<sub>18</sub>H<sub>29</sub>NO<sub>4</sub>: C, 66.86; H, 9.26; N, 4.32. Found: C, 66.91; H, 9.30; N, 4.29.

**2-Isobutyltricyclo[3.3.1.1<sup>3,7</sup>]decan-2-amine (8).** Tertiary alcohol **19** was obtained after treating a solution of 2-adamantanone **12** (500 mg, 3.34 mmol) in dry THF (5 mL) with isobutyllithium (8 mL, 10.02 mmol, 1.6 M in hexanes) at 0 °C in a 1:3 ratio as before: yield 85%; <sup>1</sup>H NMR (CDCl<sub>3</sub>, 400 MHz)  $\delta$  0.96 (d, *J* = 7 Hz, 6H, 2 × CH<sub>3</sub>), 1.52 (d, *J* = 12 Hz, 2H, 4'eq, 9'eq-H), 1.57 (d, *J* = 6 Hz, 2H, CH<sub>2</sub>CHMe<sub>2</sub>), 1.66 (1',3',6'-H), 1.68–1.74 (m, 2H, 8'eq, 10'eq-H), 1.78 (br s, 2H, 5',7'-H), 1.76–1.87 (m, 1H, CH<sub>2</sub>CHMe<sub>2</sub>), 1.82 (d, *J* = 12 Hz, 2H, 8'ax, 10'ax-H), 2.16 (d, *J* = 12 Hz, 2H, 4'ax, 9'ax-H); <sup>13</sup>C NMR (CDCl<sub>3</sub>, 50 MHz)  $\delta$  23.2 (2 × CH<sub>3</sub>), 25.3 (CH<sub>2</sub>CHMe<sub>2</sub>), 27.5 (5',7'-C), 35.1 (4',9'-C), 33.1 (8',10'-C), 37.6 (1',3'-C), 38.5 (6'-C), 46.5 (CH<sub>2</sub>CHMe<sub>2</sub>), 75.9 (2'-C). The corresponding azide **26** was prepared from the alcohol **19** (300 mg, 1.44 mmol) according to the same procedure followed for azide **25** using CH<sub>2</sub>Cl<sub>2</sub> (30 mL)/NaN<sub>3</sub> (280 mg, 4.32 mmol)/TFA (1.6 mg, 14.4 mmol): yield 95%; IR (Nujol)  $\nu$ (N<sub>3</sub>) 2095 cm<sup>-1</sup>; <sup>13</sup>C NMR (CDCl<sub>3</sub>, 50 MHz) 23.4 (2 × CH<sub>3</sub>), 24.5 (CH<sub>2</sub>CHMe<sub>2</sub>), 27.3 (5',7'-C), 33.9 (4',9'-C), 33.6 (8',10'-C), 34.7 (1',3'-C), 38.5 (6'-C), 43.0 (CH<sub>2</sub>CHMe<sub>2</sub>), 69.7 (2'-C).

The corresponding oily amine **8** was prepared through LiAlH<sub>4</sub> (183 mg, 4.80 mmol) reduction of azide **26** (280 mg, 1.20 mmol) in refluxing ether for 5 h according to the same procedure followed for amine **7**: yield 65%; <sup>1</sup>H NMR (CDCl<sub>3</sub>, 400 MHz)  $\delta$  0.94 (d, *J* = 7 Hz, 6H, 2 × CH<sub>3</sub>), 1.49 (d, *J* = 6 Hz, 2H, CH<sub>2</sub>CHMe<sub>2</sub>), 1.52–1.65 (m, 2H, 1',3',6',4'eq, 9'eq-H), 1.73–1.83 (m, 1H, CH<sub>2</sub>CHMe<sub>2</sub>), 1.75 (br s, 2H, 5',7'-H), 1.95 (d, *J* = 12 Hz, 2H, 8'ax, 10'ax-H), 2.05 (d, *J* = 12 Hz, 2H, 4'ax, 9'ax-H); <sup>13</sup>C NMR (CDCl<sub>3</sub>, 50 MHz)  $\delta$  23.4 (2 × CH<sub>3</sub>), 25.7 (CH<sub>2</sub>CHMe<sub>2</sub>), 27.6 (5',7'-C), 34.3 (4',9'-C), 33.1 (8',10'-C), 38.0 (1',3'-C), 39.1 (6'-C), 47.4 (CH<sub>2</sub>CHMe<sub>2</sub>), 55.4 (2'-C). Fumarate: mp 225 °C (EtOH–Et<sub>2</sub>O). Anal. Calcd for C<sub>18</sub>H<sub>29</sub>NO<sub>4</sub>: C, 66.86; H, 9.26; N, 4.32. Found: C, 66.91; H, 9.30; N, 4.29.

**2-*n*-Hexyltricyclo[3.3.1.1<sup>3,7</sup>]decan-2-amine (9).** Tertiary alcohol **20** was obtained after the reaction of *n*-hexyllithium with 2-adamantanone **12** (500 mg, 3.34 mmol) in dry THF (5 mL) with *n*-hexyllithium (4 mL, 10.02 mmol, 2.47 M in hexanes) at 0 °C in a 1:3 ratio as before: yield 97%; IR (Nujol)  $\nu$ (OH) 3391 cm<sup>-1</sup>; <sup>1</sup>H NMR (CDCl<sub>3</sub>, 400 MHz)  $\delta$  0.87 (t, *J* = 7 Hz, 3H, CH<sub>3</sub>), 1.24–1.33 (m, 8H, CH<sub>2</sub>(CH<sub>2</sub>)<sub>4</sub>CH<sub>3</sub>), 1.51–1.54 (d, *J* = 12 Hz, 2H, 4'eq, 9'eq-H), 1.60–1.64 (m, 2H, CH<sub>2</sub>(CH<sub>2</sub>)<sub>4</sub>CH<sub>3</sub>), 1.66–1.69 (m, 6H, 1',3',6', 5',7'-H), 1.78–1.81 (d, *J* = 11 Hz, 2H, 8'ax, 10'ax-H), 2.14–2.17 (d, *J* = 12 Hz, 2H, 4'ax, 9'ax-H); <sup>13</sup>C NMR (CDCl<sub>3</sub>, 50 MHz)  $\delta$  14.2 ((CH<sub>2</sub>)<sub>4</sub>CH<sub>3</sub>), 22.1 ((CH<sub>2</sub>)<sub>4</sub>CH<sub>3</sub>), 22.7 ((CH<sub>2</sub>)<sub>3</sub>CH<sub>2</sub>CH<sub>2</sub>CH<sub>3</sub>), 27.4–27.6 (5',7'-C), 30.1 (CH<sub>2</sub>CH<sub>2</sub>CH<sub>2</sub>(CH<sub>2</sub>)<sub>2</sub>CH<sub>3</sub>), 32.0 (CH<sub>2</sub>CH<sub>2</sub>(CH<sub>2</sub>)<sub>3</sub>CH<sub>3</sub>), 33.1 (4',9'-C), 34.7 (8',10'-C), 37.1 (1',3'-C), 38.4 (CH<sub>2</sub>(CH<sub>2</sub>)<sub>4</sub>CH<sub>3</sub>), 38.5 (6'-C), 75.1 (2'-C).

The corresponding azide **27** was prepared from the alcohol **20** (400 mg, 1.69 mmol) according to the same procedure followed for azide **25** using CH<sub>2</sub>Cl<sub>2</sub> (30 mL)/NaN<sub>3</sub> (330 mg, 5.07 mmol)/TFA (1.9 mg, 16.9 mmol): yield 91%; IR (Nujol)  $\nu$ (N<sub>3</sub>) 2088 cm<sup>-1</sup>; <sup>13</sup>C NMR (CDCl<sub>3</sub>, 50 MHz)  $\delta$  14.2 ((CH<sub>2</sub>)<sub>4</sub>CH<sub>3</sub>), 22.6 ((CH<sub>2</sub>)<sub>4</sub>CH<sub>2</sub>CH<sub>3</sub>), 22.7 (CH<sub>2</sub>)<sub>3</sub>CH<sub>2</sub>CH<sub>2</sub>CH<sub>3</sub>, 27.2–27.4 (5',7'-C), 29.9 (CH<sub>2</sub>CH<sub>2</sub>CH<sub>2</sub>(CH<sub>2</sub>)<sub>2</sub>CH<sub>3</sub>), 31.9 (CH<sub>2</sub>CH<sub>2</sub>(CH<sub>2</sub>)<sub>3</sub>CH<sub>3</sub>), 33.7 (4',9'-C), 33.8 (8',10'-C), 34.4 (1',3'-C), 35.4 (CH<sub>2</sub>(CH<sub>2</sub>)<sub>4</sub>CH<sub>3</sub>), 38.5 (6'-C), 69.7 (2'-C).

The corresponding oily amine **9** was prepared through LiAlH<sub>4</sub> (233 mg, 6.13 mmol) reduction of azide **27** (400 mg, 1.53 mmol) in refluxing ether for 5 h according to the same procedure followed for amine **7**: yield 97%; <sup>1</sup>H NMR (CDCl<sub>3</sub>, 400 MHz)  $\delta$  0.87 (t, *J* = 7 Hz, 3H, CH<sub>3</sub>), 1.24–1.30 (m, 8H, CH<sub>2</sub>(CH<sub>2</sub>)<sub>4</sub>CH<sub>3</sub>), 1.51–1.56 (m, 4H, 4'eq, 9'eq-H, CH<sub>2</sub>(CH<sub>2</sub>)<sub>4</sub>CH<sub>3</sub>), 1.57–1.67 (m, 6H, 1', 3', 6', 8'eq, 10'eq-H), 1.79 (br s, 2H, 5',7'-H), 1.93 (d, *J* = 12 Hz, 2H, 8'ax, 10'ax-H), 2.04 (d, *J* = 12 Hz, 2H, 4'ax, 9'ax-H); <sup>13</sup>C NMR (CDCl<sub>3</sub>, 50 MHz)  $\delta$  14.2 (CH<sub>3</sub>), 22.3 ((CH<sub>2</sub>)<sub>4</sub>CH<sub>2</sub>CH<sub>3</sub>), 22.8 ((CH<sub>2</sub>)<sub>3</sub>CH<sub>2</sub>CH<sub>2</sub>CH<sub>3</sub>), 27.4–27.8 (5',7'-C), 30.3 (CH<sub>2</sub>CH<sub>2</sub>CH<sub>2</sub>(CH<sub>2</sub>)<sub>2</sub>CH<sub>3</sub>), 32.0 (CH<sub>2</sub>CH<sub>2</sub>(CH<sub>2</sub>)<sub>3</sub>CH<sub>3</sub>), 33.1 (4',9'-C), 34.1 (8',10'-C), 37.4 (1',3'-C), 38.8 (CH<sub>2</sub>(CH<sub>2</sub>)<sub>4</sub>CH<sub>3</sub>), 39.1 (6'-C), 54.6 (2'-C). Fumarate: mp 225 °C (EtOH–Et<sub>2</sub>O). Anal. Calcd for C<sub>20</sub>H<sub>33</sub>NO<sub>4</sub>: C, 68.94; H, 9.46; N, 3.99. Found: C, 68.59; H, 9.55; N, 3.79.

**2-Phenyltricyclo[3.3.1.1<sup>3,7</sup>]decan-2-amine (10).** Tertiary alcohol **21** was obtained after treating a solution of adamantanone **12** (500 mg, 3.34 mmol) in dry THF (30% solution w/v) with 2 molar excess PhMgBr (obtained from bromobenzene (1.05 g, 6.68 mmol) and 1.5 molar excess of Mg (240 mg, 10.02 mmol) in 20 mL of dry ether/g bromobenzene) and stirring the mixture overnight: yield 95%; <sup>1</sup>H NMR (CDCl<sub>3</sub>, 400 MHz)  $\delta$  1.67–1.77 (m, 8H, adamantane-H), 1.89 (br s, 2H, 5',7'-H), 2.14 (s, 1H, OH), 2.40 (d, *J* = 12 Hz, 1H, 4'ax, 9'ax-H), 2.56 (br s, 2H, 1',3'-H), 7.20–7.60 (m, 5H, phenyl-H); <sup>13</sup>C NMR (CDCl<sub>3</sub>, 50 MHz)  $\delta$  27.0, 27.5 (5',7'-C), 33.1 (4',9'-C), 34.9 (8',10'-C), 35.7 (1',3'-C), 37.8 (6'-C), 75.8 (2'-C), 125.5, 127.1, 127.2, 128.8, 143.0 (Ph).

The corresponding azide **28** was prepared from alcohol **21** (300 mg, 1.31 mmol) according to the same procedure followed for azide **25** using CH<sub>2</sub>Cl<sub>2</sub> (30 mL)/NaN<sub>3</sub> (256 mg, 3.94 mmol)/TFA (1.49 mg, 13.1 mmol): yield 95%; IR (Nujol)  $\nu$ (N<sub>3</sub>) 2098 cm<sup>-1</sup>; <sup>13</sup>C NMR (CDCl<sub>3</sub>, 50 MHz)  $\delta$  26.8, 27.4 (5',7'-C), 33.1 (4',9'-C), 33.4 (8',10'-C), 34.1 (1',3'-C), 37.7 (6'-C), 70.3 (2'-C), 125.6, 127.3, 127.8, 128.9, 140.3 (Ph).

The corresponding oily amine **10** was prepared through LiAlH<sub>4</sub> (175 mg, 4.58 mmol) reduction of azide **28** (290 mg, 1.15 mmol) in refluxing ether for 5 h according to the same procedure followed for amine **7**: yield 55%; <sup>1</sup>H NMR (CDCl<sub>3</sub>, 400 MHz)  $\delta$  1.53 (br s, 2H, 6'-H), 1.61–1.80 (m, 6H, adamantane-H), 1.90 (br s, 2H, 5',7'-H), 2.33 (d, *J* = 12 Hz, 1H, 4'ax, 9'ax-H), 2.45 (br s, 2H, 1',3'-H), 7.18–7.25 (m, 5H, phenyl-H); <sup>13</sup>C NMR (CDCl<sub>3</sub>, 50 MHz)  $\delta$  27.2, 27.6 (5',7'-C), 32.9 (4',9'-C), 34.6 (8',10'-C), 35.8 (1',3'-C), 38.2 (6'-C), 57.8 (2'-C), 125.2, 126.2, 128.8, 148.7 (Ph). Hydrochloride: mp > 265 °C (EtOH–Et<sub>2</sub>O). Anal. Calcd for C<sub>16</sub>H<sub>22</sub>NCl: C, 72.85; H, 8.41; N, 5.31. Found: C, 72.81; H, 8.63; N, 5.29.

**2-Benzyltricyclo[3.3.1.1<sup>3,7</sup>]decan-2-amine (11).** Tertiary alcohol **22** was obtained after treating a solution of adamantanone **12** (500

mg, 3.34 mmol) in dry THF (30% solution w/v) with 2-molar excess  $\text{PhCH}_2\text{MgCl}$  (obtained from  $\text{PhCH}_2\text{Cl}$  (846 mg, 6.68 mmol) and 1.5 molar excess of Mg (243 mg, 10.02 mmol) in 20 mL of dry ether/g bromobenzene) and stirring the mixture overnight: yield 95%;  $^1\text{H}$  NMR ( $\text{CDCl}_3$ , 400 MHz)  $\delta$  1.51 (d,  $J = 12$  Hz, 2H, 4'eq, 9'eq-H), 1.65 (br s, 1H, 6'-H), 1.69 (br s, 1H, 5',7'-H), 1.77 (d,  $J = 12$  Hz, 2H, 8'eq, 10'eq-H), 1.78 (br s, 1H, 3'-H), 1.90 (br s, 1H, 1'-H), 2.07 (d,  $J = 12$  Hz, 1H, 8'ax, 10'ax-H), 2.12 (d,  $J = 12$  Hz, 1H, 4'ax, 9'ax-H), 2.97 (s, 2H,  $\text{CH}_2\text{Ph}$ ), 7.10–7.32 (m, 5H, phenyl-H);  $^{13}\text{C}$  NMR ( $\text{CDCl}_3$ , 50 MHz)  $\delta$  27.4, 27.5 (5',7'-C), 33.1 (4',9'-C), 34.7 (8',10'-C), 36.9 (1',3'-C), 38.5 (6'-C), 43.9 ( $\text{CH}_2\text{Ph}$ ), 74.7 (2'-C), 126.5, 128.3, 130.7, 137.4 (Ph).

The corresponding azide **29** was prepared from alcohol **22** (300 mg, 1.24 mmol) according to the same procedure followed for azide **25** using  $\text{CH}_2\text{Cl}_2$  (30 mL)/ $\text{NaN}_3$  (241 mg, 3.71 mmol)/TFA (1.41 mg, 12.4 mmol): yield 50%; IR (Nujol)  $\nu(\text{N}_3)$  2096  $\text{cm}^{-1}$ ;  $^{13}\text{C}$  NMR ( $\text{CDCl}_3$ , 50 MHz)  $\delta$  27.1, 27.4 (5',7'-C), 33.7 (4',9'-C), 33.8 (8',10'-C), 34.1 (1',3'-C), 38.4 (6'-C), 41.4 ( $\text{CH}_2\text{Ph}$ ), 69.8 (2'-C), 126.7, 128.2, 130.3, 136.6 (Ph).

The corresponding oily amine **11** was prepared through  $\text{LiAlH}_4$  (130 mg, 3.45 mmol) reduction of azide **29** (230 mg, 0.861 mmol) in refluxing ether for 5 h according to the same procedure followed for amine **7**: yield 45%;  $^1\text{H}$  NMR ( $\text{CDCl}_3$ , 400 MHz)  $\delta$  1.61 (d,  $J = 12$  Hz, 2H, 4'eq, 9'eq-H), 1.61 (br s, 1H, 6'-H), 1.73 (br s, 1H, 5',7'-H), 1.78 (d,  $J = 12$  Hz, 2H, 8'eq, 10'eq-H), 1.87 (br s, 1H, 3'-H), 1.97 (br s, 1H, 1'-H), 2.09 (d,  $J = 12$  Hz, 1H, 8'ax, 10'ax-H), 2.29 (d,  $J = 12$  Hz, 1H, 4'ax, 9'ax-H), 2.97 (s, 2H,  $\text{CH}_2\text{Ph}$ ), 7.10–7.32 (m, 5H, phenyl-H);  $^{13}\text{C}$  NMR ( $\text{CDCl}_3$ , 50 MHz)  $\delta$  27.6, 27.8 (5',7'-C), 33.2 (4',9'-C), 34.3 (8',10'-C), 37.3 (1',3'-C), 39.2 (6'-C), 44.2 ( $\text{CH}_2\text{Ph}$ ), 55.1 (2'-C), 126.3, 128.1, 130.7, 138.4 (Ph). Fumarate: mp 205 °C ( $\text{EtOH-Et}_2\text{O}$ ). Anal. Calcd for  $\text{C}_{20}\text{H}_{33}\text{NO}_4$ : C, 70.56; N, 3.92. Found: C, 70.99; N, 3.89.

**(B) Biological Testing Methods. Cells and Media.** Tissue used for preparation of virus stock cultures, virus infectivity titrations, and miniplaque drug assays were Madin–Darby canine kidney (MDCK) cells (ATCC CCL 34). The cell culture growth medium used was Dulbecco's modified Eagle medium (DMEM, Sigma-Aldrich) supplemented with 0.11% sodium bicarbonate, 5% Cosmic calf serum (Hyclone), 10 mM HEPES buffer, and 50  $\mu\text{g}/\text{mL}$  gentamycin. For culture of virus stocks and virus infectivity assays, 0.125% bovine serum albumin (BSA, Sigma-Aldrich) was substituted for the Cosmic calf serum.

**Virus.** Influenza A virus, the 2009 pandemic strain (A/California/07/2009), was provided by Dr. Don Smee, Utah State University. Trypsin added to BSA-supplemented medium for virus activation was TPCK-treated bovine pancreas trypsin (Sigma-Aldrich). A virus stock culture (passage 1) was prepared in MDCK cells in a 150  $\text{cm}^2$  culture flask. The cells were plated in growth medium and incubated until the cell monolayer was at 90% confluency. The monolayer was washed with medium containing no serum, then renewed with BSA medium containing 2.5  $\mu\text{g}/\text{mL}$  trypsin. The culture was infected with 1 mL of the virus inoculum obtained from Dr. Smee, then incubated at 33 °C. At 2 days postinfection the culture had reached complete cytopathic effect. Detached cells and cell debris were removed by low speed centrifugation (600g for 5 min). The supernate was aliquoted in 1 mL quantities, then frozen at  $-80$  °C for storage. For virus titration, aliquots of the stock were thawed and dilution series were inoculated in MDCK cultures in shell vials and virus-infected cells were detected by immunofluorescence. Other virus strains were obtained from American Type Culture Collection (ATCC): influenza A (H3N2) Victoria/3/75 (ATCC VR-822), influenza A (H1N1) A/PR/8/34 (ATCC VR-95), influenza A (H1N1) A/WS/33 (ATCC VR-1520), and influenza A (H2N2) A2/Taiwan/1/64 (ATCC VR-480). Virus stock cultures were prepared in MDCK cells grown in BSA-supplemented media, processed, and stored as described above.

For resistance studies with A/Hong Kong/1/1968 (H3N2) (Table 4), Petri dishes with MDCK cells (Federal Research Institute for Animal Health, Greifswald-Insel Riems, catalog no. RIE328) were preincubated overnight in Eagle minimum essential medium (EMEM) supplemented with 10% fetal bovine serum, 100 U/mL penicillin, and

100  $\mu\text{g}/\text{mL}$  streptomycin, and the assay compound at concentrations corresponding to 5–10 $\times$   $\text{EC}_{50}$  was determined using the CPE assay.<sup>25</sup>

**Miniplaque Assay.** In cell culture, miniplaques consist of single infected cells, double or multiple infected cells contiguously linked, that are observed microscopically and identified by immunofluorescence using FITC-labeled monoclonal antibody against viral protein. Antiviral activity of test drugs was detected in cultures exposed to drug by assessing inhibition of viral protein synthesis (virus replication) as measured by reduction in number of miniplaques. The tests were performed in MDCK cells. Cells were grown on 12 mm glass coverslips in shell vials (Sarstedt) to a cell density of 80–99% confluency in 1 mL of DMEM growth medium per vial. Prior to infection the cultures were washed with serumless media. The serumless medium was replaced with 1 mL per vial of DMEM containing BSA at a concentration of 0.125%. Test drugs at appropriate concentrations were added to the cultures and allowed to equilibrate with the media. Stock virus was thawed, and appropriate concentrations of virus (contained in BSA media) were then exposed to 1.0  $\mu\text{g}/\text{mL}$  trypsin for 30 min at room temperature, then added to the cultures. Replicate cultures were included at each dilution step of test chemical. Control cultures containing no antiviral drug were included in each assay. The cultures were then incubated at 33 °C overnight. Cultures were washed with phosphate buffered saline (PBS) within the shell vials, fixed in  $-80$  °C acetone, then stained with anti-influenza A, FITC-labeled monoclonal antibody (Millipore, Billerica, MA, USA). Possible drug toxicity in culture was assessed by microscopic observation of cytologic changes and cell multiplication rates.  $\text{EC}_{50}$  determinations were carried out with a fluorescence microscope by counting miniplaques (clusters of infected cells) in confluent MDCK monolayers on a coverslip at drug concentrations of 50, 20, 10, 5  $\mu\text{M}$ , and if necessary, 2  $\mu\text{M}$ . From two to four replicate cultures were included at each drug concentration step. Plaque counts,  $C(D)$  (including controls and weighted by the standard error of the count for each concentration), were fitted, using the Levenberg–Marquardt algorithm (in KaleidaGraph from Synergy Software, Reading, PA, USA), to the sigmoidal function:

$$C(D) = \frac{C_0}{1 + \frac{D}{\text{EC}_{50}}}$$

with  $D$  being the drug concentration and  $C_0$  and  $\text{EC}_{50}$  being free parameters. The standard error of the  $\text{EC}_{50}$ , used as reported by the software, reflects the uncertainties due to variances in the counts at all concentrations, including the controls. The value of  $C_0$  was constrained by the four independent controls. For the replicate screens, where the value of  $\text{EC}_{50}$  was based only on the four controls and a pair of tests at a fixed concentration, the formal standard errors of the parameters may not adequately represent the uncertainty associated with extrapolating or interpolating the 50% reduction dose from the miniplaque reduction at the assay dose, which would probably be greater the greater the difference is between the assay dose and the  $\text{EC}_{50}$ . Nevertheless, in spite of this limitation, we found reproducibility of  $\text{EC}_{50}$  values to be high (i.e., within factors of  $\sim 2$ ) on several occasions where experiments were repeated, either screens repeated by screens or screens compared to complete dose–response curves.

**Resistance Testing.** For Table 4, cultured MDCK cells bathed in a concentration corresponding to approximately the  $\text{EC}_{50}$  concentration were exposed to the usual quantities of virus for 3–4 days (5–7 virus replication cycles). After that time, the cultures developed cytopathic effects, and the cultures were terminated. The medium, containing virus, was then collected by low speed centrifugation. Dose–response tests utilizing the miniplaque technique were performed on the recovered virus for determination of the  $\text{EC}_{50}$  against the potentially mutated virus. An increase in the  $\text{EC}_{50}$  above the original value represents resistance development. A crude sequence on the passage-12 virus developed in **6** (see text) was carried out by extracting the virus directly with the RNAqueous kit (Life Technologies), transcribed with the Superscript III first-strand



synthesis kit (Life Technologies), amplified by PCR, and sequenced with an Applied Biosystems 3730xl DNA analyzer.

**Resistance Test Plaque Sequencing.** For the more detailed sequencing in (Supporting Information Table 1), MDCK cells were washed and incubated with influenza virus (multiplicity of infection is 1) for 1 h to allow virus adsorption. Then excessive virus was washed off and cells were incubated with EMEM supplemented with the assay compound for 3–4 days. If no cytopathic effect was visible, 0.5 mL of supernatant was centrifuged (2000 rpm) to remove cell detritus and transferred to Petri dishes with confluent MDCK monolayers (blind passage). Cells were incubated again up to 4 days in EMEM supplemented with the assay compound. If CPE was visible, 1 mL of supernatant was stored at  $-80\text{ }^{\circ}\text{C}$  and 0.5 mL was passaged. Up to 10 passages were executed. For sequencing of resistant viruses, serial dilution (10-fold) of the stocks of the first, fourth, and ninth passages were used for plaque assays. Three to five arbitrarily selected plaques of each tested passage and compound were picked, amplified in MDCK cells (yielding second, fifth, and tenth passage virus) and used for RNA preparation as described.<sup>26</sup> Briefly, total RNA was prepared from virus-infected MDCK cells using the RNeasy Mini kit and Qiashredder kit (Qiagen, Hilden, Germany). Reverse transcription was conducted with a primer specific to the 3'-end of genomic RNA (5'-RGCRAAAGCAGG-3'), 20 units reverse transcriptase (Fermentas, St. Leon-Rot, Germany), and 5  $\mu\text{g}$  of RNA in a final reaction volume of 20  $\mu\text{L}$ . Specific oligonucleotide primers Bm-M-1 and Bm-M-1027R and Bm-HA-1 and Bm-HA-rev<sup>27</sup> were used for the amplification of the M and HA segments from cDNA. Amplified DNA fragments were analyzed by agarose gel electrophoresis and gel-extracted employing the QIAquick gel extraction kit (Qiagen, Hilden, Germany). Purified DNA fragments were sequenced by cycle sequencing using the CEQ DTCS quick start kit (Beckman Coulter, Krefeld, Germany) and analyzed on a CEQ8000 sequencer (Beckman Coulter, Krefeld, Germany).

**Electrophysiology Methods.** cDNA sequences encoding the full-length A/California/04/09 M2 protein containing an N-terminal FLAG-tag plus 3(Gly) repeat linker and either N31 or an S31 mutation were cloned into pcDNA3 and transiently co-transfected with a pcDNA3 vector encoding eGFP into TSA-201 cells using standard transfection protocols (Lipofectamine 2000, Life Technologies). Single GFP-positive transfected cells were then used for electrophysiological experiments.

Macroscopic ionic currents were recorded in the whole-cell configuration 24–48 h after transfection. Cells were perfused continuously at 3–5 mL/min with external (bath) solution containing the following (in mM): 150 NMG, 10 HEPES, 10 D-glucose, 2 CaCl<sub>2</sub>, 1 MgCl<sub>2</sub> buffered at pH 7.4 with HCl. For low pH (5.5) solution, HEPES was replaced by MES. Solutions containing either K<sup>+</sup> or Na<sup>+</sup> were prepared by replacing NMG with the corresponding ion. Patch electrodes were pulled from thin-walled borosilicate glass (World Precision Instruments, Fl) and fire-polished before filling with standard pipet solution containing the following (in mM): 140 NMG, 10 EGTA, 10 MES, and 1 MgCl<sub>2</sub> buffered at pH 6.0 with HCl. Pipettes typically had a resistance of 3–5 M $\Omega$ . Voltage-clamp experiments were performed with an Axopatch 200B amplifier (Molecular Devices, CA) connected to a Digidata 1322A 16-bit digitizer. Data were acquired with the pCLAMP8.0 software (Molecular Devices, CA) sampled at 10 kHz and low-pass-filtered at 5 kHz. Cells were held at  $-40\text{ mV}$ . The standard voltage protocol consisted of a 100 ms pulse to  $-80\text{ mV}$  followed by a 300 ms ramp to  $+40\text{ mV}$  and a 200 ms step to 0 mV before stepping back to  $-40\text{ mV}$  and repeated every 4 s. All experiments were performed at room temperature (20–22  $^{\circ}\text{C}$ ). All drugs were prepared as DMSO stocks (50 or 100 mM) and diluted with external solution to the desired concentration. To measure block of M2 currents by compounds, cells were recurrently treated with pH 7.4 and pH 5.5 solutions until stable, pH-dependent inward currents were reproducibly observed, followed by treatment with compound and concentration of interest at pH 5.5 for 2–30 min. At the end of each experiment, cells were then treated with 100  $\mu\text{M}$  amantadine.

**(C) Peptide Synthesis and Sample Preparation for Solid State NMR.** S31N M2 TM (22–46) (A/Udm/307/72) with <sup>15</sup>N labeled V28, A30, and I42 was synthesized using Fmoc (9-fluorenylmethoxycarbonyl) chemistry. Fmoc-[<sup>15</sup>N]Val, fmoc-[<sup>15</sup>N]Ala, and fmoc-[<sup>15</sup>N]Ile were purchased from Cambridge Isotope Laboratory (Andover, MA). Solid-phase 0.25 mmol syntheses of M2 TMD were performed on an Applied Biosystems 430A peptide synthesizer as previously described.<sup>28</sup> The peptide was cleaved from the resin by the treatment with ice cold 95% TFA, 2.5% H<sub>2</sub>O, 1.25% ethanedithiol, 1.25% thioanisole and precipitated from TFA using ice cold ether. Following centrifugation, the supernatant was discarded and the pellet was washed with cold ether again. The precipitated peptide was dried under vacuum. Peptide purity and identity were confirmed using ESI mass spectrometry (positive ion mode).

<sup>15</sup>N-V<sub>28</sub>A<sub>30</sub>I<sub>42</sub> S31N M2 TMD was co-dissolved in trifluoroethanol (TFE) with 1,2-dimyristoyl-*sn*-glycero-3-phosphocholine (DMPC) in a 1:30 molar ratio. The solvent was removed under a stream of nitrogen gas to yield a lipid film and then dried to remove residual organic solvent under vacuum for 12 h. Thoroughly dried lipid film was hydrated with 8 mL of 10 mM HEPES buffer at pH 7.5 to form multilamellar vesicles containing M2 TMD in tetrameric state. This suspension was bath sonicated, dialyzed against 2 L of HEPES 10 mM, pH 7.5, buffer for 1 day and centrifuged at 196000g to harvest unilamellar proteoliposomes. The pellet was resuspended in a 1 mL aliquot of the decanted supernatant containing compound 6, resulting in a 1:6 molar ratio of the M2 TMD tetramer to drug. Following overnight incubation at 37  $^{\circ}\text{C}$ , the pellet was deposited on  $5.7 \times 10\text{ mm}$  glass strips (Matsunami Trading, Osaka, Japan). The bulk of the water from the sample was removed during a 2-day period in a 98% relative humidity environment at 298 K. Rehydration of the slides, before stacking and sealing into a rectangular sample cell, generated 40–50% by weight water in the sample. The final sample composition is 1 mg of drug/60 mg of lipid/8 mg of peptide (mole ratio 1:20:0.7) with 40–50% hydration.

**Solid State NMR Experiments.** PISEMA spectra were acquired at 720 MHz utilizing a low-E <sup>1</sup>H/<sup>15</sup>N double resonance probe.<sup>28,29</sup> Acquisition took place at 303 K, above the gel to liquid crystalline phase transition temperature of DMPC lipids. Experimental parameters included a 90° pulse of 5  $\mu\text{s}$  and cross-polarization contact time of 1 ms, a 4 s recycle delay, and a SPINAL decoupling sequence.<sup>30</sup> Sixteen  $t_1$  increments were obtained for the spectrum of <sup>15</sup>N-V<sub>28</sub>A<sub>30</sub>I<sub>42</sub> S31N M2 TMD with compound 6, and nine  $t_1$  increments were obtained for the sample without compound. Spectral processing was done with NMRPIPE<sup>31</sup> and plotting with SPARKY. <sup>15</sup>N chemical shifts were referenced to a concentrated solution of N<sub>2</sub>H<sub>8</sub>SO<sub>4</sub>, defined as 26.8 ppm relative to liquid ammonia.

## ■ ASSOCIATED CONTENT

### 📄 Supporting Information

Plaque hemagglutinin-sequencing results, plaque M1-sequencing results, plaque M2-sequencing results, and representative diary plots from tSA-201 HEK cells. This material is available free of charge via the Internet at <http://pubs.acs.org>.

## ■ AUTHOR INFORMATION

### Corresponding Authors

\*A.K.: phone, 30-210-727-4834; e-mail, [ankol@pharm.uoa.gr](mailto:ankol@pharm.uoa.gr).

\*D.D.B.: phone, 801-422-8753; e-mail, [david\\_busath@byu.edu](mailto:david_busath@byu.edu).

### Author Contributions

A.K. and C.T. synthesized compounds. F.B.J. and R.Z. did dose–response and resistance tissue-culture testing. T.A.C. and A.K.W. did solid state NMR. I.T. and D.F. did electrophysiology tests. A.K. and D.D.B. conceived and supervised the project and wrote the paper with input from the coauthors.

### Notes

The authors declare no competing financial interest.

## ACKNOWLEDGMENTS

The authors thank Dr. Donald Smee for providing influenza A/California/07/2009 (H1N1) and Dr. Michaela Schmidtke for her collaboration and her valuable suggestions. D.D.B. thanks Curtis Evans, Steven Kearnes, Nathan Gay, Ben Nielsen, Trevor Anderson, Robert Childs, and Joseph Moulton. R.Z. thanks Birgit Jahn and Martina Müller, and D.F. thanks Daniel Kwan for technical assistance. The work is part of C.T.'s Master's thesis and was supported by grants from Chiesi Hellas (Project 10354, Special Account for Research Grants), the German Ministry for Education and Science (FluResearchNet, Grant 01 KI1006J), and NIH (Grants AI 23007 and AI 074805).

## REFERENCES

- (1) Bright, R. A.; Medina, M. J.; Xu, X.; Perez-Orozco, G.; Wallis, T. R.; Davis, X. M.; Povinelli, L.; Cox, N. J.; Klimov, A. I. Incidence of adamantane resistance among influenza A (H3N2) viruses isolated worldwide from 1994 to 2005: a cause for concern. *Lancet* **2005**, *366*, 1175–1181.
- (2) (a) Bright, R. A.; Shay, D. K.; Shu, B.; Cox, N. J.; Klimov, A. I. Adamantane resistance among influenza A viruses isolated early during the 2005–2006 influenza season in the United States. *JAMA, J. Am. Med. Assoc.* **2006**, *295*, 891–894. (b) Lan, Y.; Zhang, Y.; Dong, L.; Wang, D.; Huang, W.; Xin, L.; Yang, L.; Zhao, X.; Li, Z.; Wang, W.; Li, X.; Xu, C.; Guo, J.; Wang, M.; Peng, Y.; Gao, Y.; Guo, Y.; Wen, L.; Jiang, T.; Shu, Y. A comprehensive surveillance of adamantane resistance among human influenza A virus isolated from mainland China between 1956 and 2009. *Antiviral Ther.* **2010**, *15*, 853–859.
- (3) High levels of adamantane resistance among influenza A (H3N2) viruses and interim guidelines for use of antiviral agents—United States, 2005–06 influenza season. *Morbidity Mortality Wkly. Rep.* **2006**, *55*, 44–46.
- (4) See, for examples, the following: (a) Kolocouris, N.; Foscolos, G. B.; Kolocouris, A.; Marakos, P.; Pouli, N.; Fytas, G.; Ikeda, S.; De Clercq, E. Synthesis and antiviral activity evaluation of some aminoadamantane derivatives. *J. Med. Chem.* **1994**, *37*, 2896–2902. (b) Kolocouris, A.; Spearpoint, P.; Martin, S. R.; Hay, A. J.; Lopez-Querol, M.; Sureda, F. X.; Padalko, E.; Neyts, J.; De Clercq, E. Comparisons of the influenza virus A M2 channel binding affinities, anti-influenza virus potencies and NMDA antagonistic activities of 2-alkyl-2-aminoadamantanes and analogues. *Bioorg. Med. Chem. Lett.* **2008**, *18*, 6156–6160.
- (5) (a) Stouffer, A. L.; Acharya, R.; Salom, D.; Levine, A. S.; Di Costanzo, L.; Soto, C. S.; Tereshko, V.; Nanda, V.; Stayrook, S.; DeGrado, W. F. Structural basis for the function and inhibition of an influenza virus proton channel. *Nature* **2008**, *451*, 596–599. (b) Cady, S. D.; Schmidt-Rohr, K.; Wang, J.; Soto, C. S.; DeGrado, W. F.; Hong, M. Structure of the amantadine binding site of influenza M2 proton channels in lipid bilayers. *Nature* **2010**, *463*, 689–692. (c) Cady, S. D.; Wang, J.; Wu, Y.; DeGrado, W. F.; Hong, M. Specific binding of adamantane drugs and direction of their polar amines in the pore of the influenza M2 transmembrane domain in lipid bilayers and dodecylphosphocholine micelles determined by NMR spectroscopy. *J. Am. Chem. Soc.* **2011**, *133*, 4274–4284. (d) Pielak, R. M.; Oxenoid, K.; Chou, J. J. Structural investigation of rimantadine inhibition of the AM2-BM2 chimera channel of influenza viruses. *Structure* **2011**, *19*, 1655–1663. (e) Hu, J.; Fu, R.; Cross, T. A. The chemical and dynamical influence of the anti-viral drug amantadine on the M2 proton channel transmembrane domain. *Biophys. J.* **2007**, *93*, 276–283.
- (6) Wang, J.; Wu, Y.; Ma, C.; Fiorin, G.; Pinto, L. H.; Lamb, R. A.; Klein, M. L.; DeGrado, W. F. Structure and inhibition of the drug-resistant S31N mutant of the M2 ion channel of influenza A virus. *Proc. Natl. Acad. Sci. U.S.A.* **2013**, *110*, 1315–1320.
- (7) Scholtissek, C.; Quack, G.; Klenk, H. D.; Webster, R. G. How to overcome resistance of influenza A viruses against adamantane derivatives. *Antiviral Res.* **1998**, *37*, 83–95.
- (8) Kurtz, S.; Luo, G.; Hahnenberger, K. M.; Brooks, C.; Gecha, O.; Ingalls, K.; Numata, K.; Krystal, M. Growth impairment resulting from expression of influenza virus M2 protein in *Saccharomyces cerevisiae*: identification of a novel inhibitor of influenza virus. *Antimicrob. Agents Chemother.* **1995**, *39*, 2204–2209.
- (9) (a) Balannik, V.; Wang, J.; Ohigashi, Y.; Jing, X.; Magavern, E.; Lamb, R. A.; DeGrado, W. F.; Pinto, L. H. Design and pharmacological characterization of inhibitors of amantadine-resistant mutants of the M2 ion channel of influenza A virus. *Biochemistry* **2009**, *49*, 696–708. (b) Duque, M. D.; Ma, C.; Torres, E.; Wang, J.; Naesens, L.; Juarez-Jimenez, J.; Camps, P.; Luque, F. J.; DeGrado, W. F.; Lamb, R. A.; Pinto, L. H.; Vazquez, S. Exploring the size limit of templates for inhibitors of the M2 ion channel of influenza A virus. *J. Med. Chem.* **2011**, *54*, 2646–2457. (c) Wang, J.; Ma, C.; Fiorin, G.; Carnevale, V.; Wang, T.; Hu, F.; Lamb, R. A.; Pinto, L. H.; Hong, M.; Klein, M. L.; DeGrado, W. F. Molecular dynamics simulation directed rational design of inhibitors targeting drug-resistant mutants of influenza A virus M2. *J. Am. Chem. Soc.* **2011**, *133*, 12834–12841. (d) Rey-Carrizo, M.; Torres, E.; Ma, M.; Barniol-Xicota, M.; Wang, J.; Wu, Y.; Naesens, L.; DeGrado, W. F.; Lamb, R. A.; Pinto, L. H.; Vázquez, S. 3-Azatetracyclo[5.2.1.1<sup>5,8</sup>.0<sup>1,5</sup>]undecane derivatives: from wild-type inhibitors of the M2 ion channel of influenza A virus to derivatives with potent activity against the V27A mutant. *J. Med. Chem.* **2013**, *56*, 9265–9274.
- (10) (a) Zhang, W. Heterodimers of histidine and amantadine as inhibitors for wild type and mutant M2 channels of influenza A. *Chin. J. Chem.* **2010**, *28*, 1417–1423. (b) Shibnev, V. A.; Garayev, T. M.; Finogenova, M. P.; Shevchenko, E. S.; Burtseva, E. I. New adamantane derivatives and ways of overcoming the resistance of influenza A viruses to rimantadine and amantadine. *Vopr. Virusol.* **2011**, *56*, 36–39. (c) Zhao, X.; Jie, Y.; Rosenberg, M. R.; Wan, J.; Zeng, S.; Cui, W.; Xiao, Y.; Li, Z.; Tu, Z.; Casarotto, M. G.; Hu, W. Design and synthesis of pinanamine derivatives as anti-influenza A M2 ion channel inhibitors. *Antiviral Res.* **2012**, *96*, 91–99. (d) Shibnev, V. A.; Garaev, T. M.; Finogenova, M. P.; Shevchenko, E. S.; Burtseva, E. I. New adamantane derivatives can overcome resistance of influenza A(H1N1)pdm2009 and A(H3N2) viruses to rimantadine. *Bull. Exp. Biol. Med.* **2012**, *153*, 233–235. (e) Torres, E.; Fernández, R.; Miquet, S. P.; Font-Bardia, M.; Vanderlinden, E.; Naesens, L.; Vázquez, S. Synthesis and anti-influenza A virus activity of 2,2-dialkylamantadines and related compounds. *ACS Med. Chem. Lett.* **2012**, *3*, 1065–1069. (f) Wang, J.; Ma, C.; Jo, H.; Canturk, B.; Fiorin, G.; Pinto, L. H.; Lamb, R. A.; Klein, M. L.; DeGrado, W. F. Discovery of novel dual inhibitors of wild-type and the most prevalent drug-resistant mutant, S31N, of M2 proton channel from influenza A virus. *J. Med. Chem.* **2013**, *56*, 2804–2812. (g) Torres, E.; Duque, M. D.; Vanderlinden, E.; Ma, C.; Pinto, L. H.; Camps, P.; Froeyen, M.; Vazquez, S.; Naesens, L. Role of the viral hemagglutinin in the anti-influenza virus activity of newly synthesized polycyclic amine compounds. *Antiviral Res.* **2013**, *99*, 281–291.
- (11) Kalir, A.; Balderman, D. *Org. Synth.* **1981**, *60*, 104–107.
- (12) Sasaki, T.; Eguchi, S.; Toi, N. Synthesis of adamantane derivatives. 47. Photochemical synthesis of 4-azahomoadamant-4-enes and further studies on their reactivity in some cycloadditions. *J. Org. Chem.* **1979**, *44*, 3711–3715.
- (13) Wang, J.; Denny, J.; Tian, C.; Kim, S.; Mo, Y.; Kovacs, F.; Song, Z.; Nishimura, K.; Gan, Z.; Fu, R.; Quine, J. R.; Cross, T. A. Imaging membrane protein helical wheels. *J. Magn. Reson.* **2000**, *144*, 162–167.
- (14) Hu, J.; Asbury, T.; Achuthan, S.; Li, C.; Bertram, R.; Quine, J. R.; Fu, R.; Cross, T. A. Backbone structure of the amantadine-blocked trans-membrane domain M2 proton channel from influenza A virus. *Biophys. J.* **2007**, *92*, 4335–4343.
- (15) Li, C.; Qin, H.; Gao, F. P.; Cross, T. A. Solid-state NMR characterization of conformational plasticity within the transmembrane domain of the influenza A M2 proton channel. *Biochim. Biophys. Acta* **2007**, *1768*, 3162–3170.

- (16) (a) Chizhnikov, I. V.; Geraghty, F. M.; Ogden, D. C.; Hayhurst, A.; Antoniou, M.; Hay, A. J. Selective proton permeability and pH regulation of the influenza virus M2 channel expressed in mouse erythroleukaemia cells. *J. Physiol.* **1996**, *494*, 329–336. (b) Balannik, V.; Carnevale, V.; Fiorin, G.; Levine, B. G.; Lamb, R. A.; Klein, M. L.; DeGrado, W. F.; L Pinto, L. H. Functional studies and modeling of pore-lining residue mutants of the influenza A virus M2 ion channel. *Biochemistry* **2010**, *49*, 696–708.
- (17) Appleyard, G. Amantadine-resistance as a genetic marker for influenza viruses. *J. Gen. Virol.* **1977**, *36*, 249–255.
- (18) Oxford, J. S.; Potter, C. W.; Logan, I. S. Passage of influenza strains in the presence of aminoadamantane. *Ann. N.Y. Acad. Sci.* **1970**, *173*, 300–313.
- (19) Hayden, F. G.; Sperber, S. J.; Belshe, R. B.; Clover, R. D.; Hay, A. J.; Pyke, S. Recovery of drug-resistant influenza A virus during therapeutic use of rimantadine. *Antimicrob. Agents Chemother.* **1991**, *35*, 1741–1747.
- (20) Hay, A. J.; Wolstenholme, A. J.; Skehel, J. J.; Smith, M. H. The molecular basis of the specific anti-influenza action of amantadine. *EMBO J.* **1985**, *4*, 3021–3024.
- (21) Gamblin, S. J.; Haire, L. F.; Russell, R. J.; Stevens, D. J.; Xiao, B.; Ha, Y.; Vasisht, N.; Steinhauer, D. A.; Daniels, R. S.; Elliot, A.; Wiley, D. C.; Skehel, J. J. The structure and receptor binding properties of the 1918 influenza hemagglutinin. *Science* **2004**, *303*, 1838–1842.
- (22) Shibata, M.; Aoki, H.; Tsurumi, T.; Sugiura, Y.; Nishiyama, Y.; Suzuki, S.; Maeno, K. Mechanism of uncoating of influenza B virus in MDCK cells: action of chloroquine. *J. Gen. Virol.* **1983**, *64*, 1149–1156.
- (23) Dudleemajil, E.; Lin, C. Y.; Dredge, D.; Murray, B. K.; Robison, R. A.; Johnson, F. B. Bovine parvovirus uses clathrin-mediated endocytosis for cell entry. *J. Gen. Virol.* **2010**, *91*, 3032–3041.
- (24) Kuehn, B. M. CDC: Use antivirals early, aggressively for H7N9 flu. *JAMA, J. Am. Med. Assoc.* **2013**, *309*, 2086.
- (25) Schmidtke, M.; Schnittler, U.; Jahn, B.; Dahse, H. M.; Stelzner, A. A rapid assay for evaluation of antiviral activity against coxsackievirus B3, influenza virus A, and herpes simplex virus type 1. *J. Virol. Methods* **2001**, *95*, 133–143.
- (26) Krumbholz, A.; Schmidtke, M.; Bergmann, S.; Motzke, S.; Bauer, K.; Stech, J.; Dürrwald, R.; Wutzler, P.; Zell, R. High prevalence of amantadine resistance among circulating European porcine influenza A viruses. *J. Gen. Virol.* **2009**, *90*, 900–908.
- (27) Hoffmann, E.; Stech, J.; Guan, Y.; Webster, R. G.; Perez, D. R. Universal primer set for the full-length amplification of all influenza A viruses. *Arch. Virol.* **2001**, *146*, 2275–2289.
- (28) Kovacs, F. A.; Cross, T. A. Transmembrane four-helix bundle of influenza A M2 protein channel: structural implications from helix tilt and orientation. *Biophys. J.* **1997**, *73*, 2511–2517.
- (29) Wu, C. H.; Ramamoorthy, A.; Opella, S. J. High-resolution heteronuclear dipolar solid-state NMR spectroscopy. *J. Magn. Reson.* **1994**, *109*, 270–272.
- (30) Fung, B. M.; Khitrin, A. K.; Ermolaev, K. An improved broadband decoupling sequence for liquid crystals and solids. *J. Magn. Reson.* **2000**, *142*, 97–101.
- (31) Delaglio, F.; Grzesiek, S.; Vuister, G. W.; Zhu, G.; Pfeifer, J.; Bax, A. NMRPipe: a multidimensional spectral processing system based on UNIX pipes. *J. Biomol. NMR* **1995**, *6*, 277–293.